

AD-A251 606



92-14924



1 92 6 05 054

EMA-91-R-001
FINAL

EMA ELECTRO MAGNETIC APPLICATIONS, INC.

P.O. Box 260263
Denver, CO 80226-2091
(303) 980-0070

EVALUATION OF THE EUROSHIELD 4F-130 RF LEAK DETECTORS

Prepared by

Dr. James R. Elliott
Henry S. Weigel

VIEWS, OPINIONS, AND/OR FINDINGS
CONTAINED IN THIS REPORT ARE THOSE OF
THE AUTHOR(S) AND SHOULD NOT BE
CONSTRUED AS AN OFFICIAL DEPARTMENT
OF THE ARMY POSITION, POLICY, OR
DECISION UNLESS SO DESIGNATED BY
OTHER OFFICIAL DOCUMENTATION.

Prepared for

Harry Diamond Laboratories
2800 Powder Mill Road
Adelphi, Maryland 20783

Under Prime Contract No.: DAAL02-90-C-0005

January 14, 1991



Accesion For	
NTIS	CRA&I
DTIC	TAB
Unannounced	
Justification	
By <i>per Ltr</i>	
Distribution /	
Availability Codes	
Dist	Avail and/or Special
A-1	

TABLE OF CONTENTS

Chapter	Title	Page
	EXECUTIVE SUMMARY	iv
1	INTRODUCTION	1
	1.1 Overview and Objectives	1
	1.2 Leak Detector Description	1
2	DIGITAL READOUT MODIFICATION	5
	2.1 Task Objectives	5
	2.2 Design and Implementation	5
	2.2.1 Digital Panel Meter	6
	2.2.2 Operating Frequency Display	6
	2.2.3 Control Switches	7
	2.3 Parts, Circuit and Construction Details	7
	2.4 Receiver Recalibration and Display Verification	13
	2.4.1 Recalibration Using Digital Display	13
	2.4.2 Display Verification	14
3	DYNAMIC RANGE AND NOISE FLOOR EVALUATION	15
4	RESPONSE LINEARITY AND ACCURACY	
	4.1 E-3 Comparison to Eaton Calibrated Receiver	20
	4.2 Comparison of Other Euroshield Leak Detectors to E-3	20
5	MEASUREMENT REPEATABILITY	33
	5.1 Repeatability of E-3 Measurement in a Precise Geometry	33
	5.2 Variations of Shelter SE Measurements 33	
6	IMPACT OF ENVIRONMENT UPON MEASUREMENTS	42
7	SUMMARY AND CONCLUSIONS	49
	7.1 Summary	49
	7.2 Other Observations	49
	7.3 Conclusions	50
	APPENDIX A - IMPACT OF OPERATOR AND TEST GEOMETRY UPON MEASUREMENT	A-1
	A.1 Operator Influence	A-2
	A.2 Calibration Location and Test Point Geometry Influences on SE	A-2
	A.2.1 The Effects of Images	A-2
	A.2.2 Calibration and Measurement	A-3

LIST OF FIGURES

Figure	Title	Page
1.1	Euroshield RF Leak Detector 4F-130	2
1.2	Measuring in Accordance to MIL-STD-285	4
2.1	Outline of Digital Display Mounting Plate	8
2.2	Printed Circuit Board Layout for Digital Display (Front and Back)	9
2.3	Circuit for Digital Display Upgrade	11
2.4	Wire Lengths for Digital Display Connector	12
2.5	Signal Description for Digital Display Connector	13
3.1	SE Noise Limit	16
3.2	SE Noise Limit Defined as 3 Standard Deviations Below Average SE Reading	17
3.3	Magnetic Field Generated by Transmitter	18
3.4	Magnetic Fields	19
4.1	E-3 vs Eaton SE, .010 MHz	21
4.2	E-3 vs Eaton SE, .156 MHz	22
4.3	E-3 vs Eaton SE, 1.00 MHz	23
4.4	E-3 vs Eaton SE, 10.0 MHz	24
4.5	E-3/Eaton Linearity Comparison, .010 MHz	25
4.6	E-3/Eaton Linearity Comparison, .156 MHz	26
4.7	E-3/Eaton Linearity Comparison, 1.00 MHz	27
4.8	E-3/Eaton Linearity Comparison, 10.0 MHz	28
4.9	Comparison of E-1 to E-3	29
4.10	Comparison of E-4 to E-3	30
4.11	Comparison of E-5 to E-3	31
4.12	Comparison of E-1 to itself at Different Time	32
5.1	E-3 Repeatability Comparison, Separation at .010 MHz	34
5.2	E-3 Repeatability Comparison, Separation at .156 MHz	35
5.3	E-3 Repeatability Comparison, Separation at 1.00 MHz	36
5.4	E-3 Repeatability Comparison, Separation at 10.0 MHz	37

LIST OF FIGURES (CONT'D.)

<u>Figure</u>	<u>Title</u>	<u>Page</u>
5.5	SE Comparison, .010 MHz	38
5.6	SE Comparison, .156 MHz	39
5.7	SE Comparison, 1.00 MHz	40
5.8	SE Comparison, 10.0 MHz	41
6.1	Temperature Dependence, .010 MHz	44
6.2	Temperature Dependence, .156 MHz	45
6.3	Temperature Dependence, 1.00 MHz	46
6.4	Temperature Dependence, 10. MHz	47
6.5	Temperature Dependence, Shelter at .156 MHz	48
A.1	Loop Perpendicular to Ground Plane, Theory	A-4
A.2	Loop Parallel to Ground Plane, Theory	A-5
A.3	Ground Plane Effects, Axes Perpendicular to Ground	A-6
A.4	Ground Plane Effects, Axes Parallel to Ground	A-7
A.5	Concrete Ground, Axes Perpendicular	A-8
A.6	Concrete Ground, Axes Parallel	A-9
A.7	Shelter Geometry SE Effect, .156 MHz	A-11

LIST OF TABLES

<u>Table</u>	<u>Title</u>	<u>Page</u>
1.1	Specifications - Euroshield RF Leak Detector 4F-130	3
1.2	Transmitter Currents	4
2.1	Digital Display Parts	10
6.1	Temperature - Humidity Combinations	42

EXECUTIVE SUMMARY

EUROSHIELD OY of Finland offers a 4F-130 RF Leak Detector for the determination of the electromagnetic shielding effectiveness (SE) of enclosures. The measurement protocol employed for this purpose is the magnetic loop test of MIL-STD-285. This report gives the results of a study of the performance of these instruments.

Four leak detectors (transmitter/receiver pairs) were evaluated. The first phase of the study consisted of the design, construction and installation of a sample and hold digital readout in the place of the original analog display. Next, linearity and absolute value of SE measurements were compared to those obtained using a calibrated EMI receiver. This was done directly or indirectly for each of the four detector sets. Generally the leak detectors performed quite well in these tests.

Repeatability of measurement values was examined with time, operator, geometry and environment as variables. Agreement among the SE's determined in different conditions was good when the test conditions were rigidly controlled. When the more usual methods of MIL-STD-285 with different operators were used, the resulting SE's had a noticeable larger spread.

A small investigation was made of the effect of test point location and how nearby conducting planes can influence the SE's obtained. The effect of images of the sources tend to decrease SE values when the loop axes are parallel to nearby conducting planes and to increase SE values when the loop axes are perpendicular to such planes. These results are summarized in an Appendix.

CHAPTER 1

INTRODUCTION

1.1 Overview and Objectives

Military tactical shelters often have the requirement of hardness to various electromagnetic environments. To verify this hardness it is necessary to characterize the shelter's EM responses to known excitations. The quantity commonly used in this characterization is the shelter's shielding effectiveness (SE). Although there are many definitions of shielding effectiveness, MIL-STD-285 is a widely used test protocol for determining SE.

A difficulty with the MIL-STD-285 evaluation procedure is its requirement of instrumentation which is heavy, bulky and expensive. Recently radio frequency (RF) leak detection systems whose designs mitigate some of these drawbacks have become commercially available. One promising unit is the Euroshield RF Leak Detector 4F-130. The work described in this report concerns a series of tests in order to understand the performance of these instruments. For these purposes five leak detector sets were purchased. Four of them were used in the performance studies described herein. They are later referred to as E-1, E-3, E-4 and E-5.

The evaluation effort covered several different phases of instrument performance. The reporting of the results is organized as follows:

1. Description of the Euroshield RF Leak Detector 4F-130
2. Installation of a sample and hold digital readout
3. Determination of dynamic range and noise floor of the leak detectors
4. Linearity and absolute accuracy of the leak detectors
5. Measurement repeatability and unit variation
6. Instrument performance at different temperatures and humidities
7. Operator, geometry and materials influence upon measurements
8. Summary and conclusions

1.2 Leak Detector Description

The Euroshield RF Leak Detector 4F-130 is manufactured in Finland by EUROSHIELD OY (tel. +358 38 50631). The detectors are available from Ralph Aronson & Associates of Stamford, CT for approximately \$7000 per set. A set consists of a transmitter and a receiver. Each of these units is battery powered and easily handheld.

Figure 1.1 shows the overall form of the two units of the set. Four discrete test frequencies, 10 kHz, 156 kHz, 1MHz and 10 MHz, are used. The measurement protocol is that of the magnetic loop test of MIL-STD-285 (Fig. 1.2) in which the near field of a magnetic dipole serves as the EM excitation. Both the transmitter and the receiver have a electrostatically shielded loop antenna which can be folded when not in use. Table 1.1 lists some of the specifications of the leak detection system.

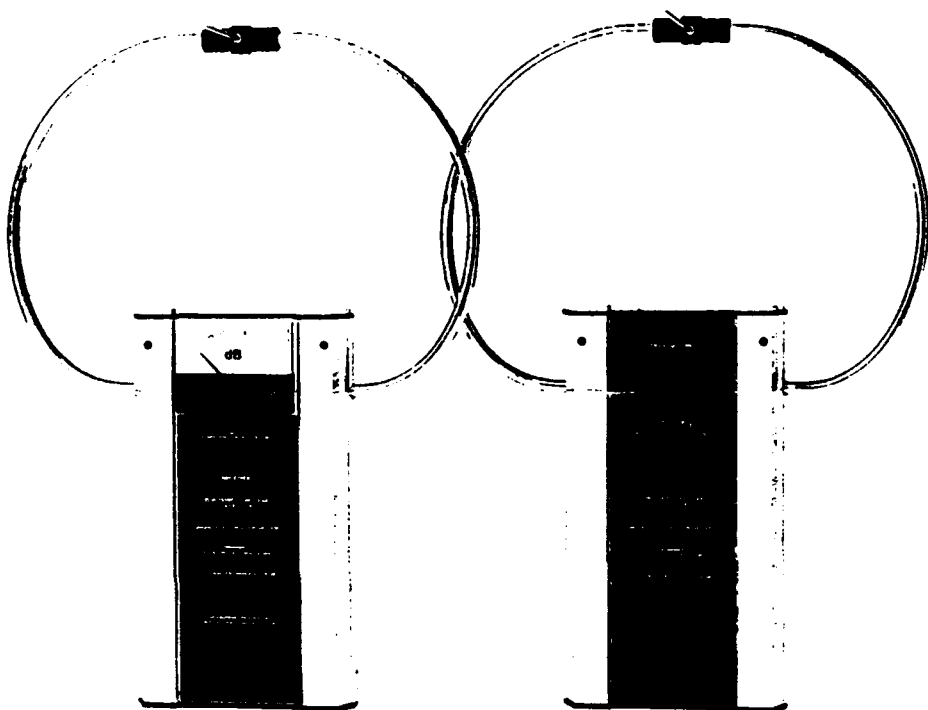


Figure 1.1 Euroshield RF Leak Detector 4F-130

Both the transmitter and the receiver have several turns of wire within the loop shield. These are used in different combinations at the various frequencies to achieve maximum dynamic range. The transmitter currents at the four frequencies are listed in Table 1.2.

When the transmitter/receiver pair is calibrated at the standard free field separation, a microprocessor evaluates and stores the signal strength for future reference. The signal measured at a test point is subtracted [in units of dB] from this free field value, yielding a direct readout of SE in dB. An 8 bit ADC samples the intermediate frequency amplifier signal and an FFT is used to find the peak value. It is claimed that this also reduces the effects of oscillator drift between the transmitter and the receiver.

Table 1.1
Specifications - Euroshield RF Leak Detector 4F-130

Frequency Range:	10.165 kHz
	156.085 kHz
	1.000165 MHz
	9.999835 MHz
Attenuation Range:	0...130 dB
Attenuation Accuracy:	+/- 1.5 dB
Display:	Analog display
LED Indication:	Battery check
Antenna:	Electrically shielded
	12 inch (30 cm) elliptical loop
Receiver Power Supply:	6 x 1.5 volt battery
Receiver weight:	1.8 kg
Transmitter Power Supply:	6 x 1.5 volt battery
Transmitter Weight:	1.7 kg
Dimensions:	275 x 150 x 48 mm (LxWxH)
Accessories:	Carrying case, 2 pcs rods of 300 mm
Battery Life:	10 hrs.
Temperature Range:	0...+40° C
Storage Temperature:	-5...+45°C

Table 1.2
Transmitter Currents

10 MHz.....	110 mA
1 MHz.....	459 mA
150 kHz.....	800 mA
10 kHz.....	1.3 A

The display is an analog current meter which displays SE from 0 to 130 dB with scale divisions every 5 dB. This analog meter was replaced by a digital readout unit which is described in Chapter 2.

Further details can be found in the User's Guide which is included as Appendix A.

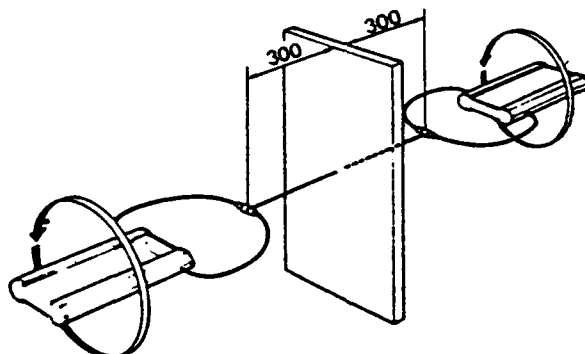


Figure 1.2 Measuring in Accordance to MIL-STD-285

CHAPTER 2

DIGITAL READOUT MODIFICATION

2.1 Task Objectives

The goal of this task was to provide a more convenient and reliable readout display of the shielding effectiveness as determined in the Euroshield receiver. A digital readout was expected to reduce error associated with operator reading and perhaps to increase the precision with which the SE reading could be made. In order to deal with measurements at constraining locations, a sample and hold feature was to be included as part of the readout modification. This would permit the detector to be held in the proper orientation during a measurement but the held SE value to be read afterwards in a more convenient manner by the operator.

This overall objective lead to several subsidiary goals for consideration in the design process:

- no adverse impact upon the functioning of the receiver,
- no compromise of the receiver's environmental integrity,
- no major change in the size or shape of the receiver,
- no compromise in the reliability or ruggedness of the receiver.

These requirements translated into several specific design constraints:

- integration of subfunctions and minimization of number of parts for display modification for reasons of both space and reliability,
- selection of parts with appropriate reliability, ruggedness and temperature range,
- use of a custom printed circuit board to meet space limitations.

2.2 Design and Implementation

A modular approach to the readout modification was adopted. The idea was to construct a separate subunit which could be located in the space of the existing analog display meter and which would be connected to the rest of the receiver only by a multi-conductor ribbon cable. Although the space available was tight, it proved possible to construct such a module.

2.2.1 Digital Panel Meter

The heart of the digital sample and hold readout module is a Modutec (Manchester, NH) "BIG-LITTLE" digital panel meter(DPM). The chosen unit has a 3 1/2 digits (.5 inch high) liquid crystal display (LCD). The DPM integrates a sampling clock, an analog to digital converter, a LCD driver, a display hold control and a backlight in a single package with 15 connectors. Some feature details are:

- 0. - 200 mV input range, even at power ground,
- adjustable reference for digital 0,
- 8 bit adc precision (~ 1/2 unit in display),
- black numerals on light background (7 segment LCD),
- polarity display (wrt to zero setting),
- green backlight (5 V), ~ 25 mA momentary,
- 2.5 samples per second,
- 100 ppm/degree C temperature coefficient,
- 9 V isolated power, < 1 mA,
- industrial temperature range -20°C - +60°C,
- environmentally sealed display, marine option.

The input which formerly went to the analog display meter was routed to the Modutec DPM. The source of this input was a digital to analog converter acting as a current source. A potentiometer controlled the gain and thus the output of this DAC for a given digital input. Fortunately, the analog meter input and the DPM input (with an appropriate 200k ohm resistor) were quite similar. Only a slight adjustment of the DAC potentiometer was required to achieve a properly calibrated response from the DPM. To facilitate this adjustment, however, the original single turn potentiometer was replaced by a precision multi-turn unit. The least count accuracy of the DPM as installed is approximately 1/2 dB.

2.2.2 Operating Frequency Display

The operating frequency display was another of the display features which was altered. In the unmodified unit, at calibration, the indicator of the analog meter jumps between the four candidate frequencies (as marked on the meter face) as it tries to determine the operating frequency of the transmitter. Upon determination of the operating frequency, the needle returns to the 0 position. Thus the last frequency indicated before the return to 0 is the operating frequency.

The approach chosen for the digital readout module was to include 4 separate light emitting diodes (LEDs). Just as with the analog display, these are illuminated sequentially, during calibration, as the receiver searches for the operating frequency. However, the LED for the operating frequency remains lit until a new calibration sequence. Since the LED draws only ~ 2 mA compared to the overall receiver use of ~120 mA, it has a very small impact on battery life.

2.2.3 Control Switches

Sample/Hold

The digital display module has two switches for the operator. The one on the right-hand side is of a toggling type. When initially pushed, it freezes the display for operator reading. Upon being pushed again, it allows the display to return to its normal mode of updating every 1/2 second.

Backlight

On the left-hand side of the digital display module is switch which controls the backlight feature of the panel meter. The backlight is an LED device which potentially draws ~100 mA. As implemented the backlight is limited to 25 mA in order to conserve power. However, even this much continuous current drain would noticeably impact battery life. Therefore, the backlight switch is of the momentary design and the backlight feature is intended for only intermittent use at the operator's convenience.

2.3 Parts, Circuit and Construction Details

The digital display module is mounted on a 1/16" thick aluminum plate with holes for the display meter, for the frequency indicating LEDs, for the control switches, for access to the zero adjustment for the meter and for the mounting screws. Its outline is shown in Figure 2.1. It is covered with a flat black enamel with white silk-screened labels. A small gasket is glued to the back of this plate to form a seal to the rest of the case of the receiver.

The two sides of the printed circuit board are shown in Figure 2.2. The panel meter, the frequency indication LEDs and the control switches are mounted directly and soldered in place to this board. After component insertion and soldering, an environmental coating seals the board. The circuit board with components is mounted to the aluminum plate described above. The original hole for the analog meter enlarged in order to permit mounting of the digital display module. This hole is just slightly larger than the circuit board.

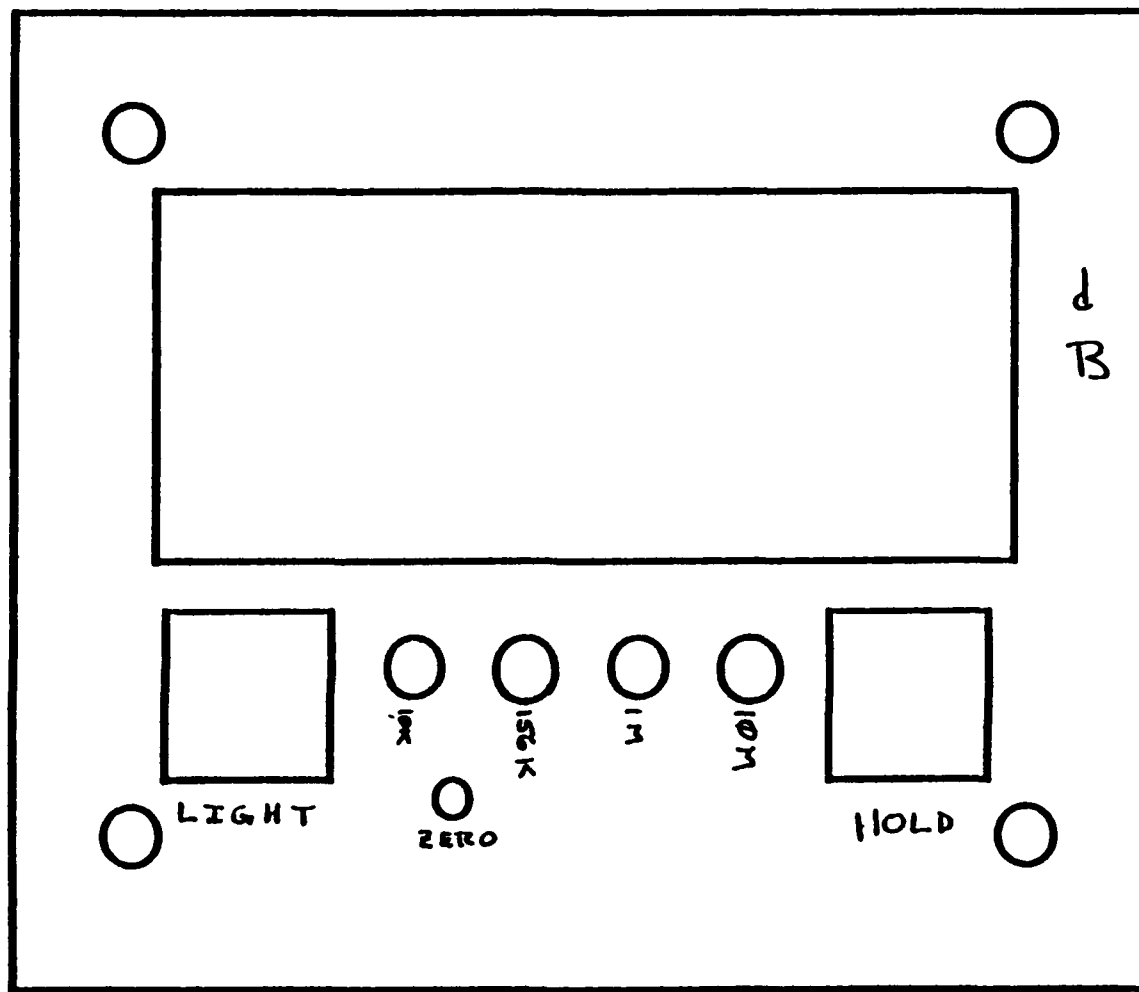


Figure 2.1 Outline of Digital Display Mounting Plate

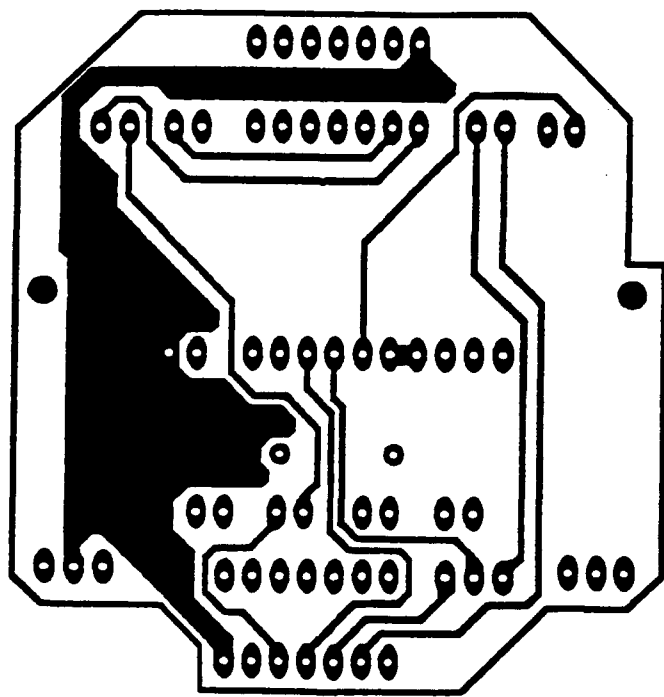
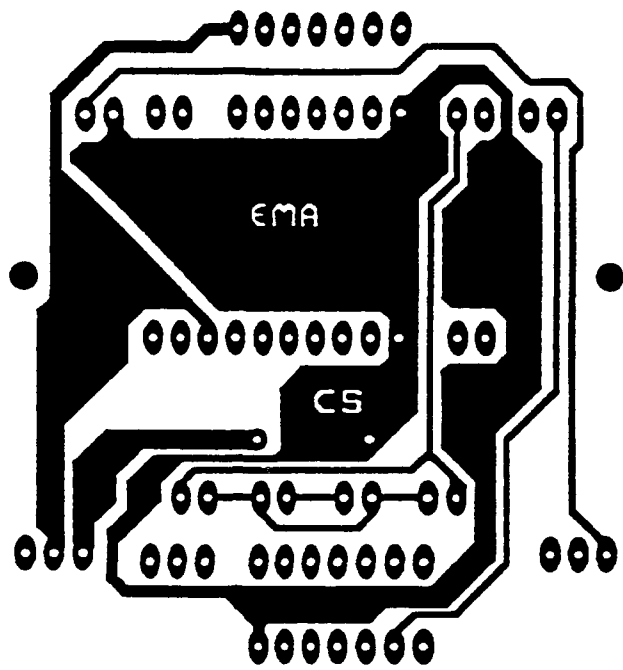


Figure 2.2 Printed Circuit Board Layout for Digital Display (Front and Back)

A circuit diagram including both the digital display module and the relevant parts of the receiver is shown in Figure 2.3. Figures 2.4 - 2.5 provide details of the cable connections between the receiver board and the digital display unit.

A parts list with source and identification information follows in Table 2.1.

Table 2.1
Digital Display Parts

Per Unit	x 10 Units	Part	Vendor	Part Number/ Catalog Page
1	10	Printed Circuit Board	Astro-Endyne	-
1	10	Aluminum Face Plate and additional machining	LaRocco Mfg.	-
1	10	Spray Painting of Plate	Front Range Spray Painting	-
1	10	Silk Screening of Plate	Precision Image Graphics	-
1	10	Modutec Display	CW Electronics	HL 330301 01 MI H 25F1490/951
4	40	LED	Newark	54LS04
1	10	Inverter IC	Arrow	P68WR500
1	10	500 Ohm Multiturn Potentiometer	CW Electronics	44F3540/219
1	10	2 k Ohm Multiturn Potentiometer	Newark	829050
1	10	50 Ohm Resistor	Fistell's	08F950/205
2	20	1.5 k Ohm Resistor	Newark	08F950/205
1	10	10 k Ohm Resistor	Newark	08F950/205
1	10	200 k Ohm Resistor	Newark	08F950/205
1	10	Backlight Switch (momentary)	Newark	23F2372/357
1	10	Hold Switch (2 pos.)	Newark	23F2471/357
2	20	Button Caps	Newark	23F2510/357
2	20	Button Models	Newark	23F2517/357
1	10	14-Pin Solder Tail Socket	Radio Shack	276-1999/124
1	10	14-Pin Dip Header Plug	Newark	56F1210/745
1 ft.	10 ft.	12-Conductor Ribbon Cable	Newark	46F4842/648
4	40	Nylon Washers	Fistell's	NW-875
1	10	Pot. Adjuster	Newark	6715775/228
4	40	Nut, Bolts and Washer	Ace Hardware	67F5795/228

Note: Newark Catalog Number 110
Radio Shack Catalog Number 459 (1991)

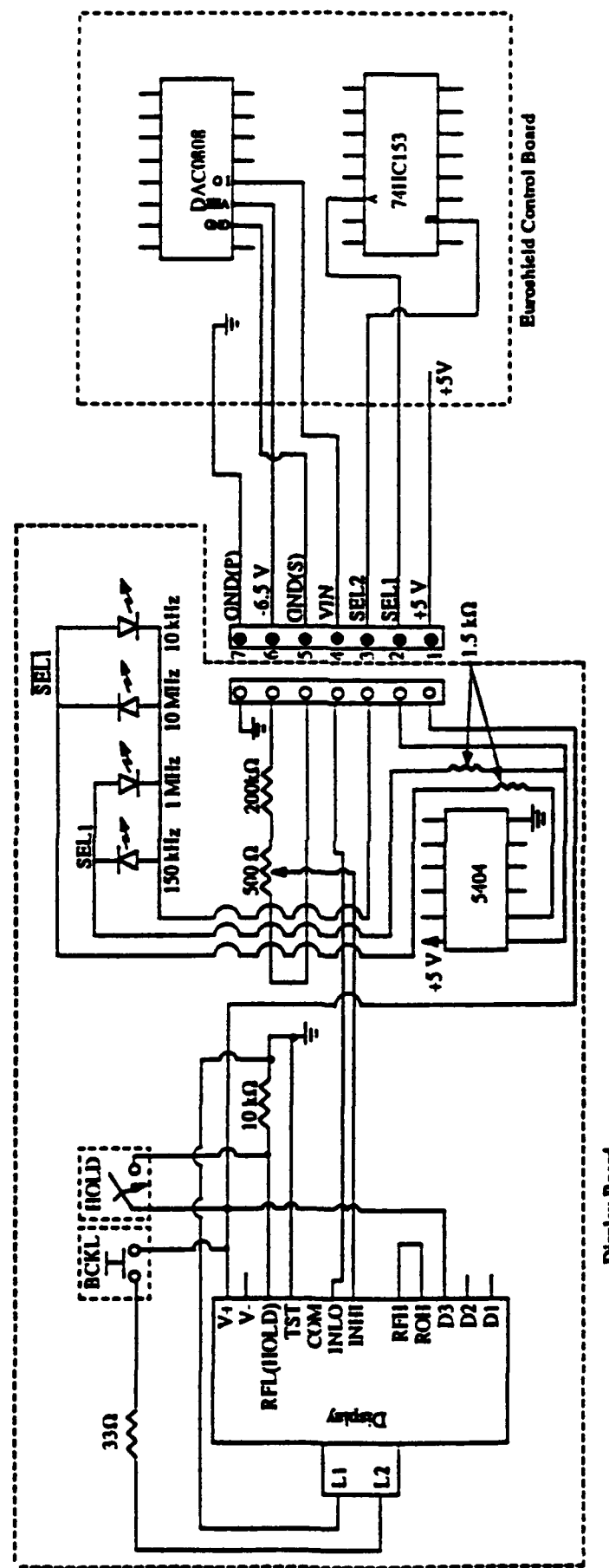


Figure 2.3 Circuit for Digital Display Upgrade

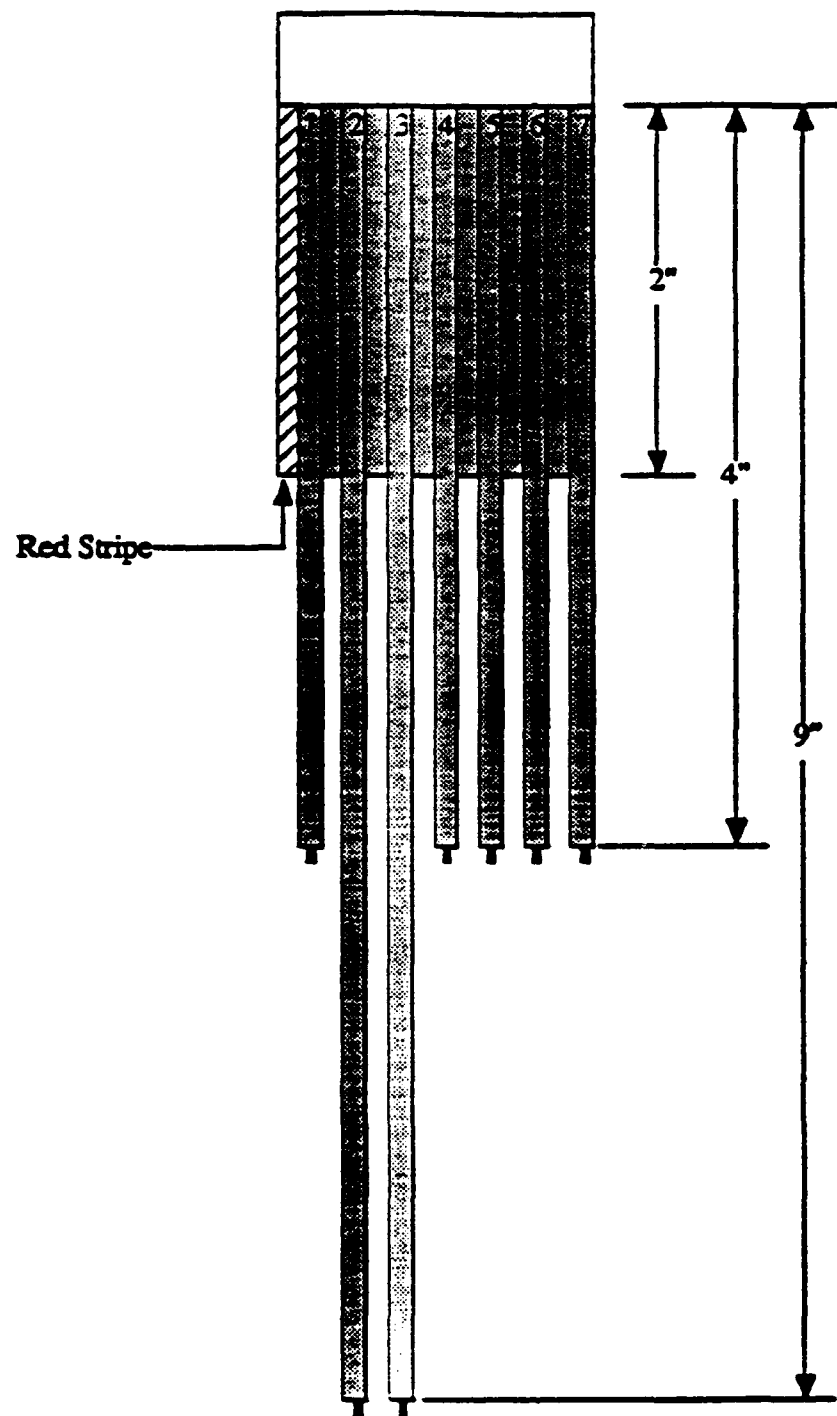


Figure 2.4 Wire Lengths for Digital Display Connector

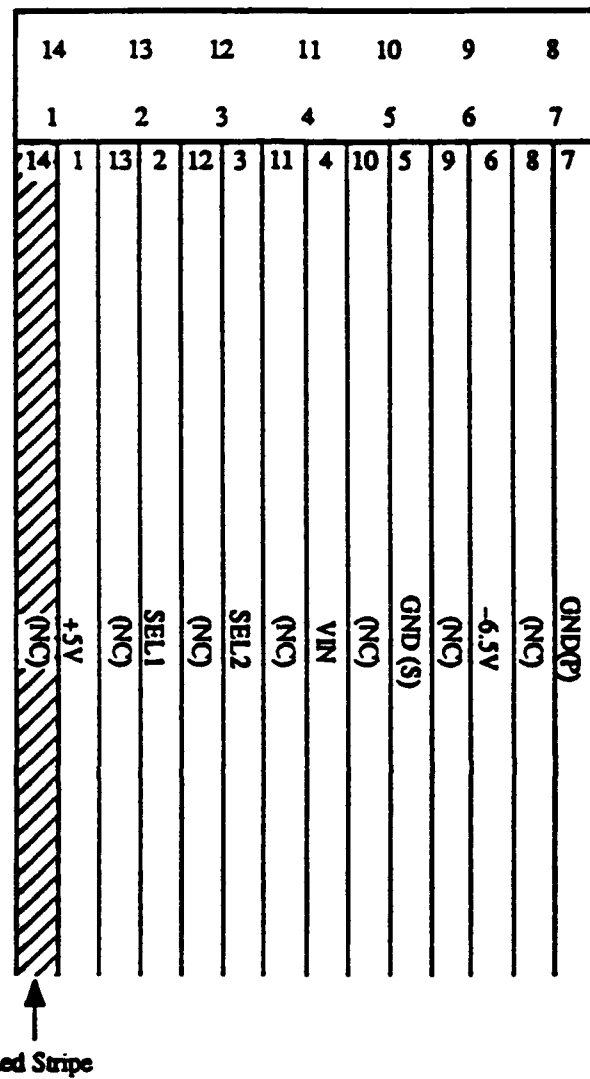


Figure 2.5 Signal Description for Digital Display Connector

2.4 Receiver Recalibration and Display Verification

2.4.1 Recalibration Using Digital Display

The first display constructed was mounted in a receiver and a calibration procedure was carried out. The steps were:

1. The Euroshield transmitter was turned on.
2. A calibrated Eaton NM 17/27 receiver with an electrostatically shielded 12 inch loop was set up in a monitoring position.
3. The Euroshield receiver with the digital display was set up in position next to the 12 inch loop such that the Euroshield loop and the 12 inch loop were equidistant from the transmitter.
4. The calibration button of the Euroshield receiver was pressed and the resulting display value was noted.
5. The zero adjustment of the digital panel meter was used to set the displayed value to 00.0.
6. The transmitter was moved away from the two receivers (along the symmetry line) until the Eaton receiver showed a decrease of approximately 70 dB.
7. The gain potentiometer of the DAC was adjusted until the displayed SE value matched the signal drop seen by the Eaton receiver.
8. The transmitter was returned to its original position and steps 4 through 7 were repeated. This set of steps was iterated until the Euroshield SE displayed agreed with Eaton decrease in signal strength without any further adjustment.

In the final calibrations, this was done only at 156 kHz. Earlier experiments at the other frequencies showed that the calibration at this frequency gave results accurate to <1 dB at the other frequencies. This also appeared to be the level of consistency between repeated measurements or recalibrations.

2.4.2 Display Verification

The first receiver converted to digital display unit was placed in an environmental chamber and temperature stabilized at 45 degrees C. It was then taken from the chamber and used to measure SE values which were also evaluated with a receiver with an analog display as well as the Eaton NM 17/27 calibrated EMI receiver. There was no significant impact upon the display function. This was repeated at a temperature of -12 degrees C. Again, no display degradation was noted. Section 6 describes more detailed tests of the leak detectors under different environmental conditions. As the remaining units were converted they were also subjected to an environmental test and comparison to the first unit.

CHAPTER 3

DYNAMIC RANGE AND NOISE FLOOR EVALUATION

3.1 Dynamic Range

The maximum measurable SE was evaluated for each of the four transmitter/receiver pairs. The procedure, for each frequency was as follows:

- perform the standard free field calibration giving SE = 0 dB,
- turn the transmitter off and take the receiver inside a shielded enclosure,
- read the SE value while inside the shielded room.

In general the SE value read in the shielded room with the transmitter off will fluctuate; this represents the inherent noise of the receiver. The sample and hold feature was used to record five successive SE values over approximately a 30 second interval. The smallest of these five values for each of the leak detector pairs at the four frequencies can be treated as the maximum dynamic range. This is valid in the sense that an actual signal registering the same SE level would be detectable by the receiver. This dynamic range is displayed in Figure 3.1.

A somewhat more sophisticated technique was also used in an alternate calculation of the maximum dynamic range. In this case average and standard deviation of a set of five readings was calculated. The dynamic range was then defined as three standard deviations below the average noise value; i.e., a SE of this level is clearly indicated without corruption by receiver noise. Figure 3.2 shows these results. The differences between Figures 3.1 and 3.2 are not great. This result was used as a guide in further data analysis in which the data is displayed for the eye and, except for simple linear fits, statistical analysis is eschewed.

3.2 Receiver Fields Levels

The Euroshield transmitter generated magnetic field levels at the receiver were measured by using a shielded 12 inch diameter loop input to an Eaton NM 17/27 calibrated receiver. From the loop area, the loop and receiver impedances and the frequency, the measured voltage was converted to a magnetic field level. This is shown in Figure 3.3 for the four frequencies. There is a balance between the frequency factor in the response and the transmitter current used at each frequency. These values are consistent with the current drives of Table 1.2 when the effects of multiple turns in the transmitter antenna are included.

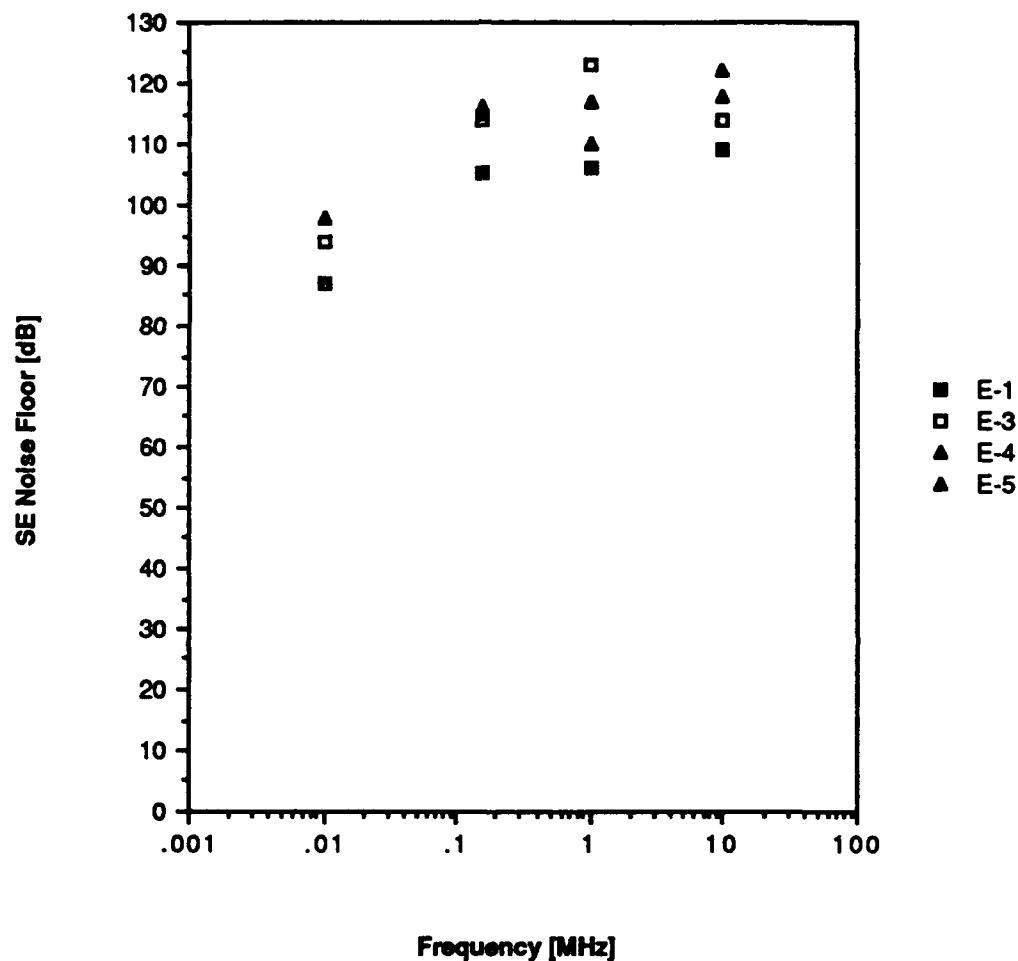


Figure 3.1 SE Noise Limit

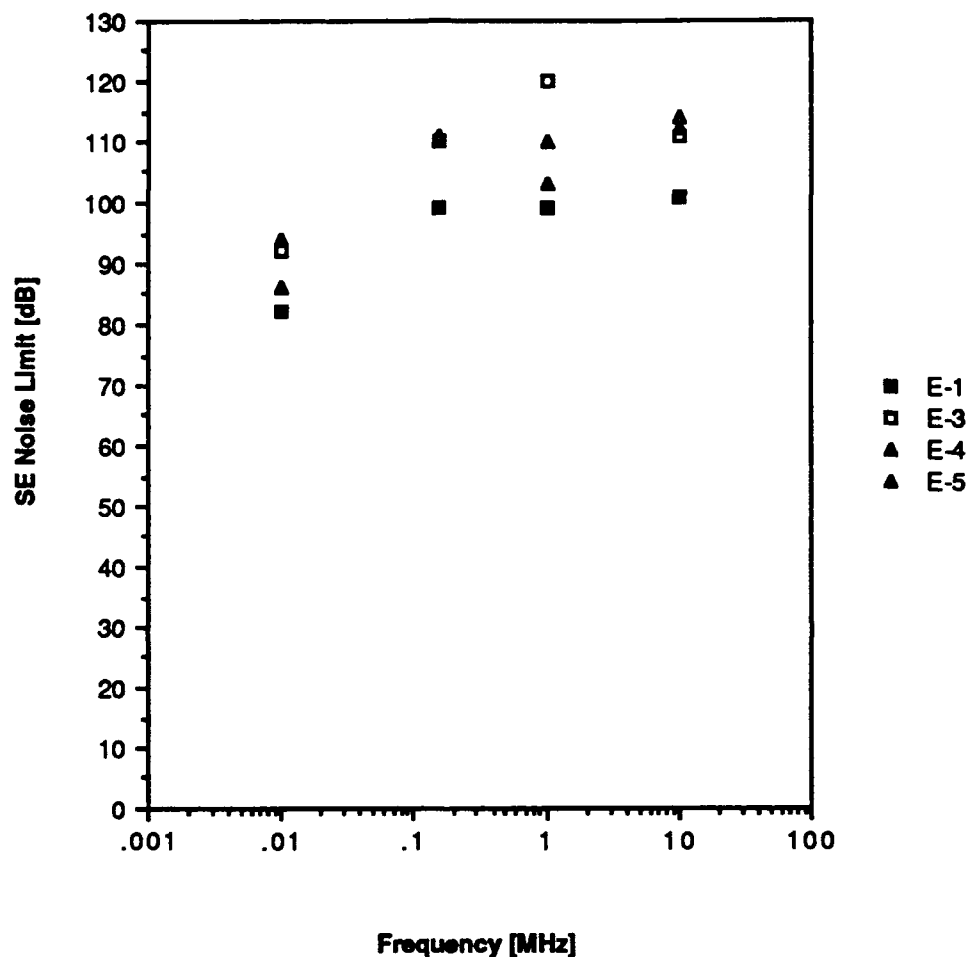


Figure 3.2 SE Noise Limit Defined as 3 Standard Deviations Below Average SE Reading

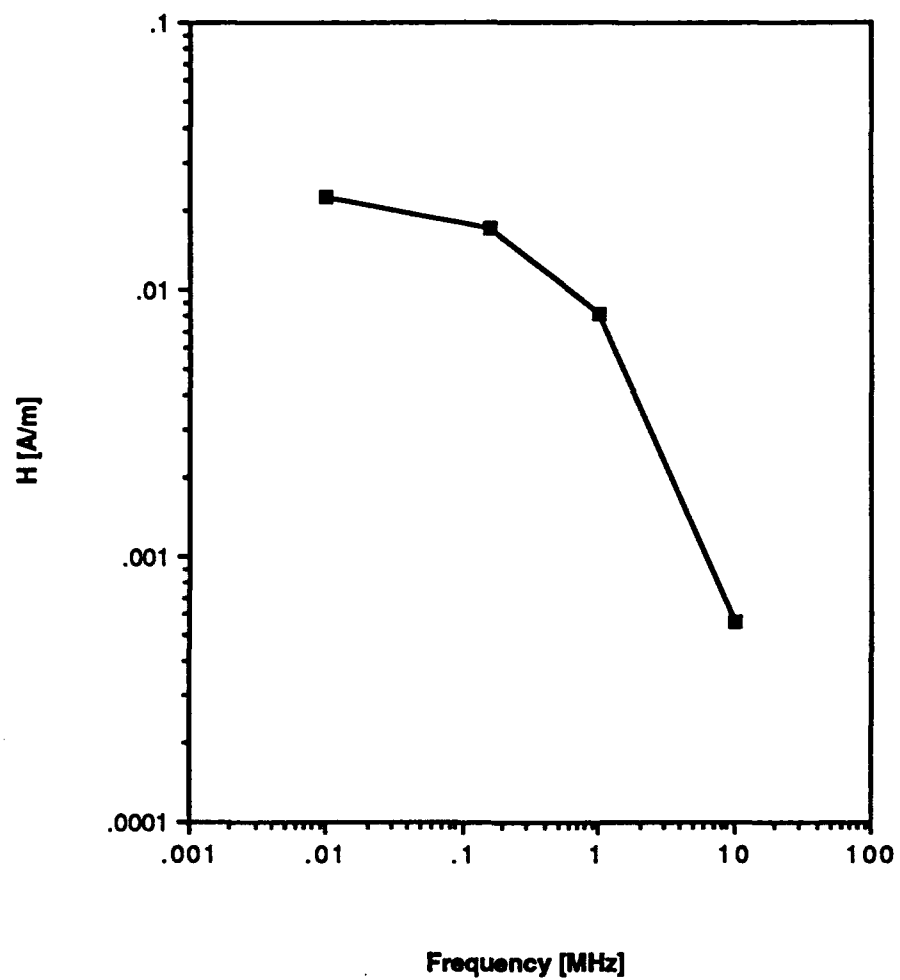


Figure 3.3 Magnetic Field Generated by Transmitter

If the transmitter was switched off, the ambient field levels in Figure 3.4 were measured. The ambient fields are well below those generated by the transmitter.

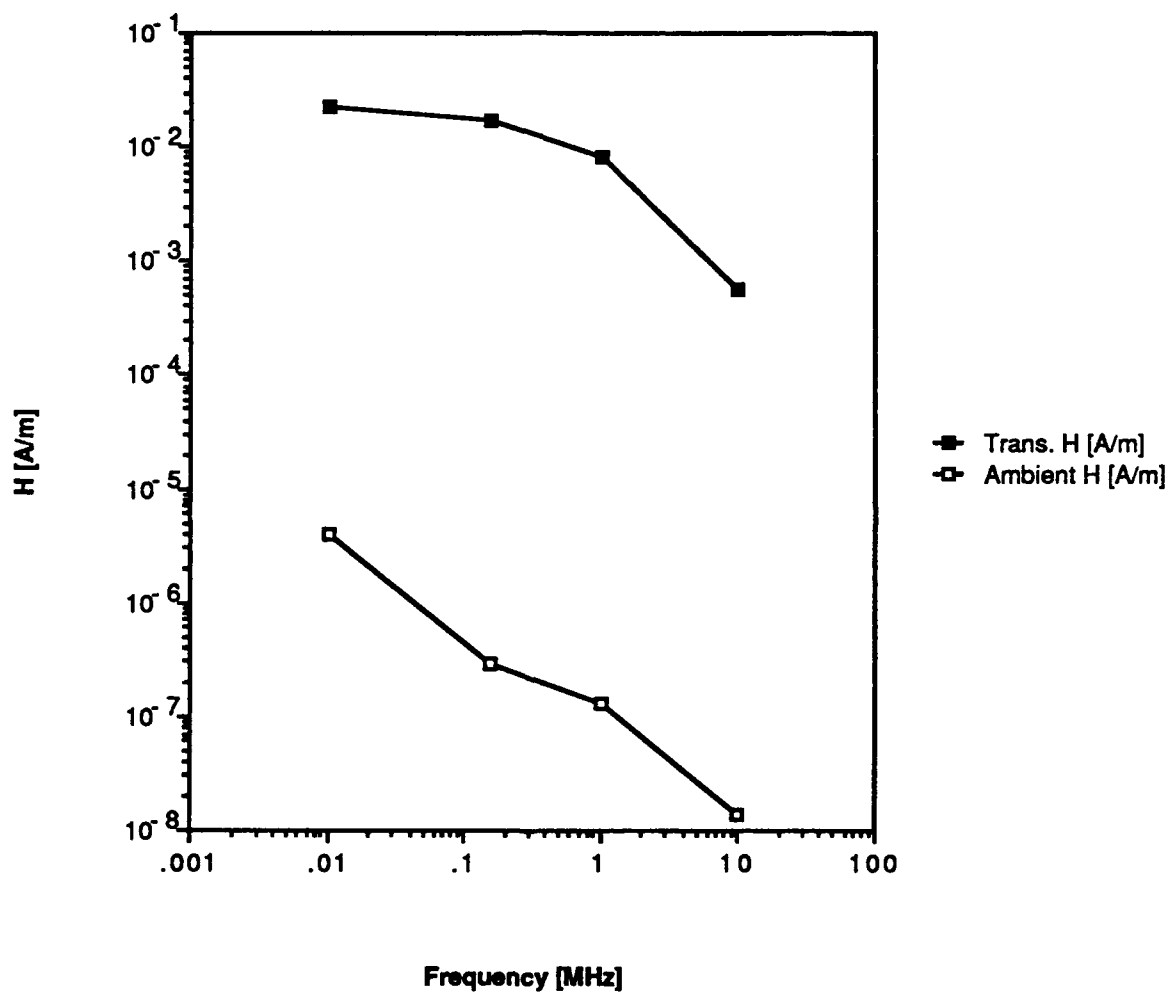


Figure 3.4 Magnetic Fields

CHAPTER 4

RESPONSE LINEARITY AND ACCURACY

4.1 E-3 Comparison to Eaton Calibrated Receiver

The display calibration technique was described in Section 2.4.1. For a check of SE linearity and absolute accuracy a variation of that technique was used. Two dielectric stands, one each for the transmitter and the receiver, were used. Six measurement locations plus the calibration position were defined. The transmitter/receiver mountings and the stand positionings could be reestablished in an accurately repeatable manner. In this way comparisons were made amongst the various Euroshield pairs as well as using a calibrated EMI receiver.

Leak detector set E-3 was used as the reference unit. It was first evaluated with respect to the Eaton receiver. In this exercise the Euroshield E-3 transmitter was used and alternately the E-3 receiver and a 12 inch shielded loop into the Eaton receiver were used. The loop separation distance at free field calibration was 26 inches. Six test locations were used at .156 MHz, while as few as three positions sufficed at the some of the other frequencies. Figures 4.1-4.4 plots the E-3 SE response versus that measured by the Eaton receiver. The response is very linear with almost unit slope and very little offset (as shown by the superimposed fitted straight line).

Figures 4.5-4.8 examines the detailed differences between the E-3 and Eaton responses. At the two lower frequencies (.010 and .156 MHz) the average error is of order .5 dB and there is very little systematic effect. At 1.0 and 10. MHz the average error is of order 1 dB with some systematic trend toward smaller values for the E-3 SE response. These are linearity and accuracy values are quite acceptable for MIL-STD-285 shelter measurements.

4.2 Comparison of Other Euroshield Leak Detectors to E-3

Because of the strong correlation of the E-3 response to that of the Eaton receiver and because of the convenience of use of the Euroshield units, E-3 was used as the reference standard for the other units, E-1, E-4 and E-5. In Figures 4.9-4.11 the SE for each pair, measured as described above, is plotted versus the E-3 SE. For comparison Figure 4.12 presents the results of a later E-3 measurement plotted versus the earlier one. The units on each axis are SE dB. E-1 and E-5 have excellent correlations to E-3 as does the E-3 remeasurement. The linear fit slopes are nearly unity and the offsets are less than .5 dB. The E-5 performance has larger deviations but of both signs. Overall, E-5 performed less well than the other units and occasionally required several attempts at calibration at 10 MHz. Still, for many MIL-STD-285 measurements E-5's results would not be significantly worse than results obtained from more traditional instrumentation.

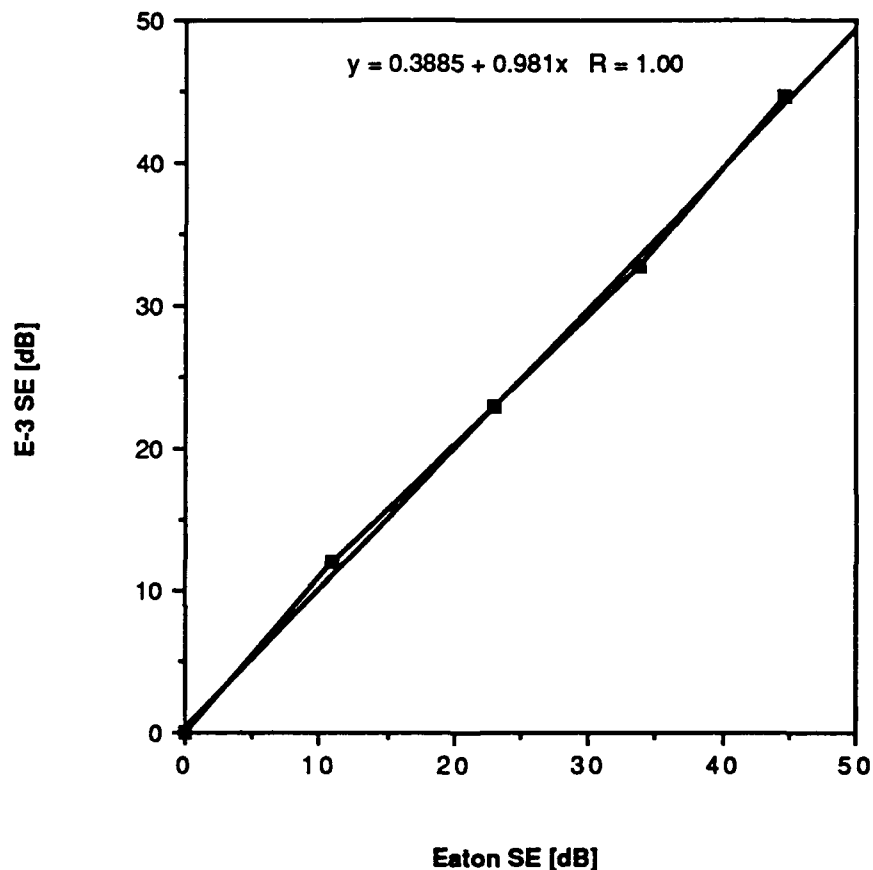


Figure 4.1 E-3 vs Eaton SE, .010 MHz

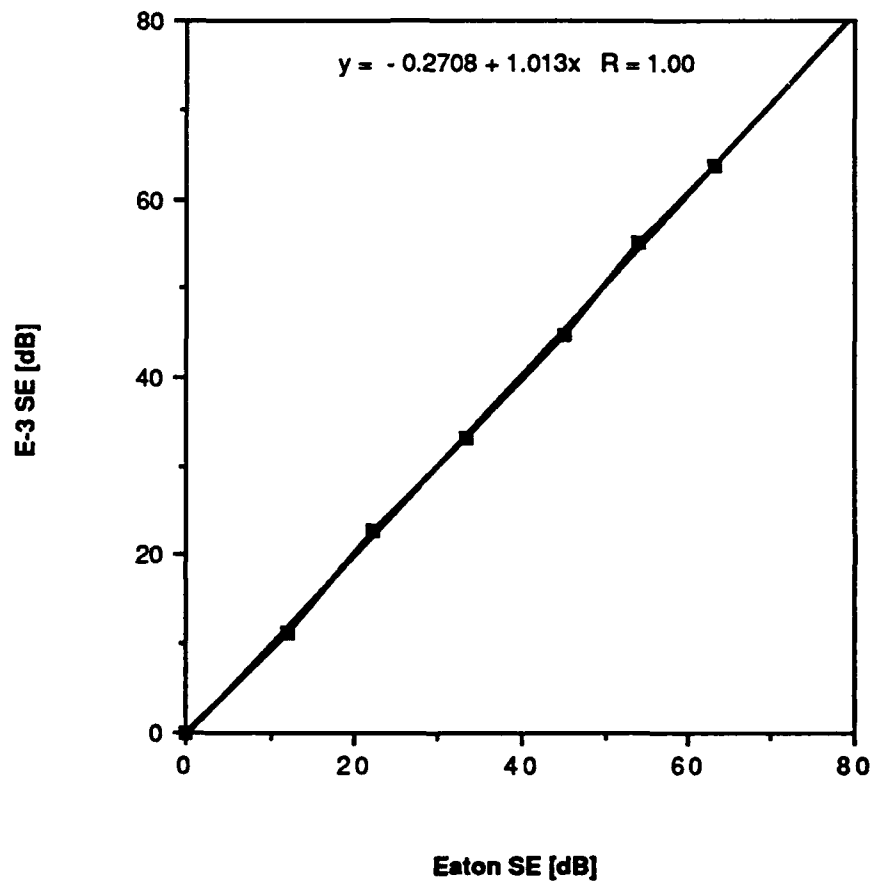


Figure 4.2 E-3 vs Eaton SE, .156 MHz

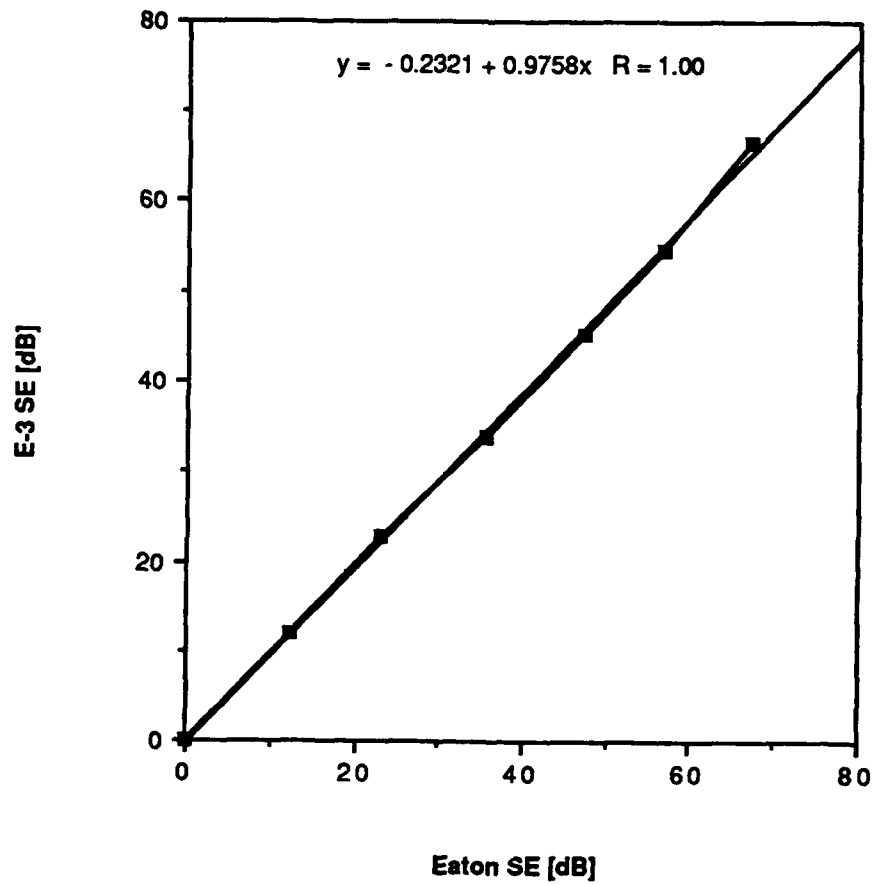


Figure 4.3 E-3 vs Eaton SE, 1.00 MHz

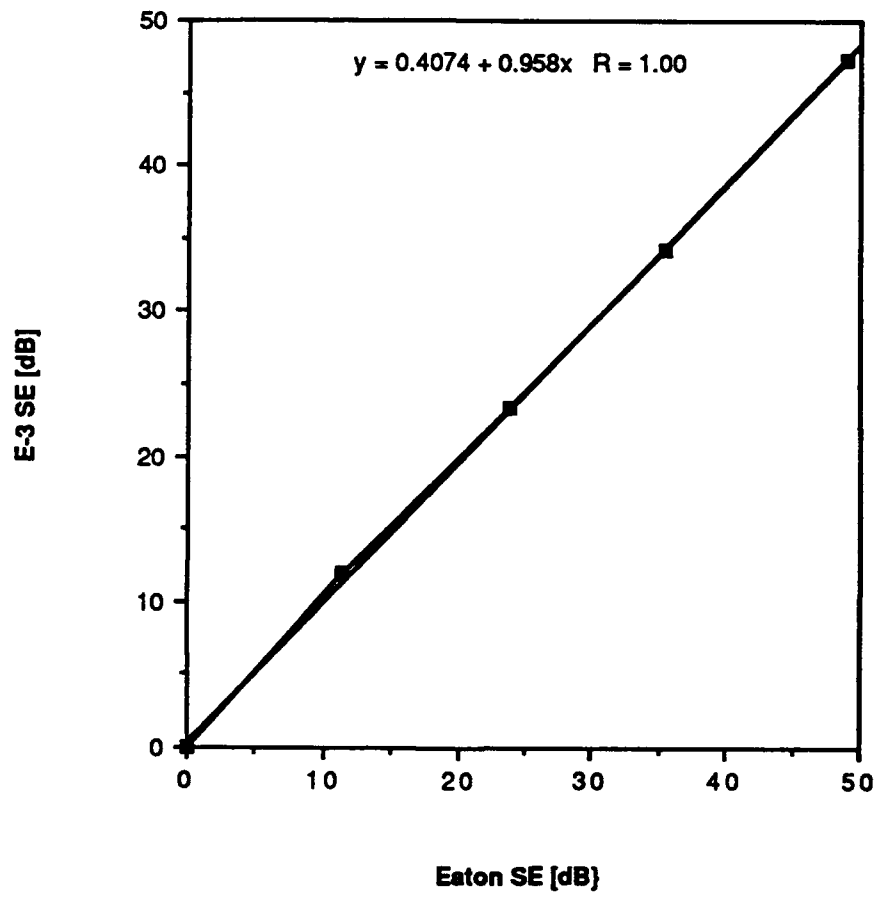


Figure 4.4 E-3 vs Eaton SE, 10.0 MHz

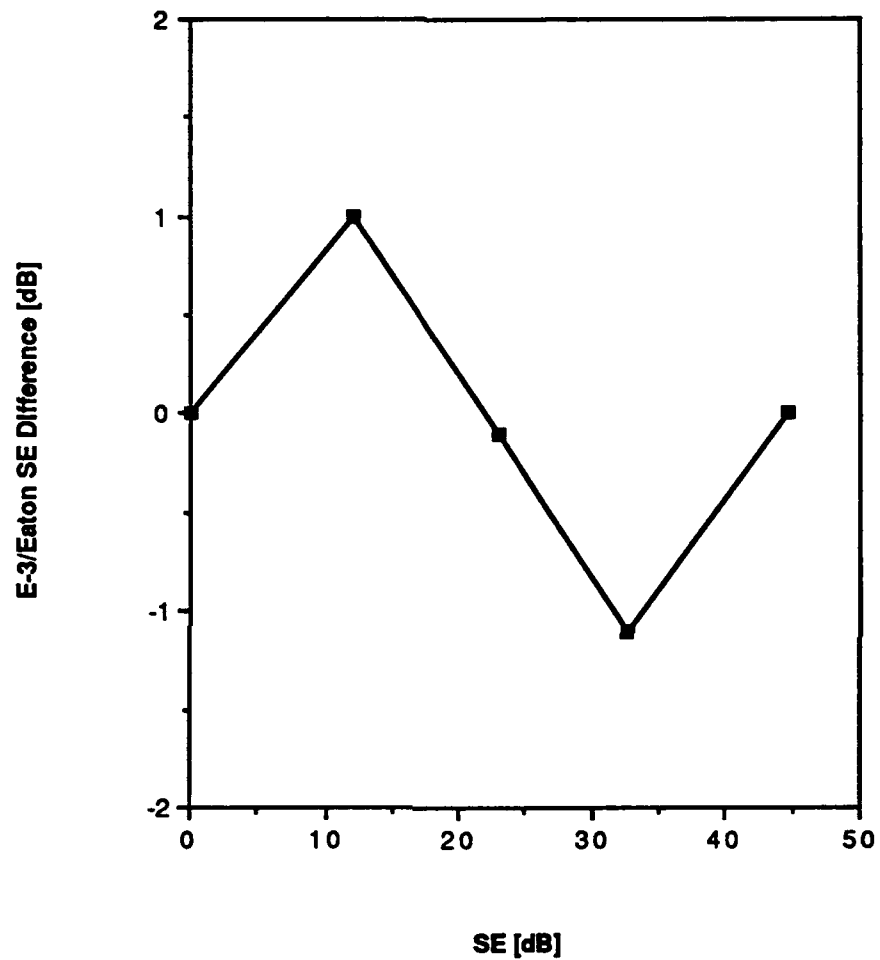


Figure 4.5 E-3/Eaton Linearity Comparison, .010 MHz

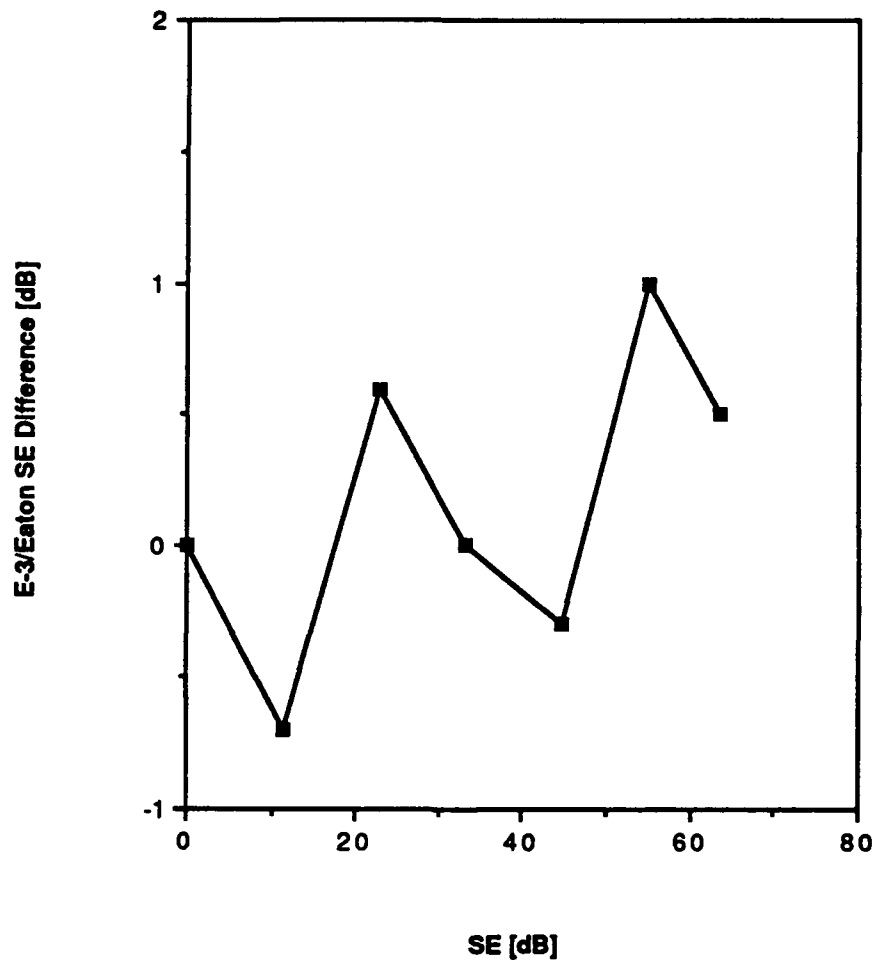


Figure 4.6 E-3/Eaton Linearity Comparison, .156 MHz

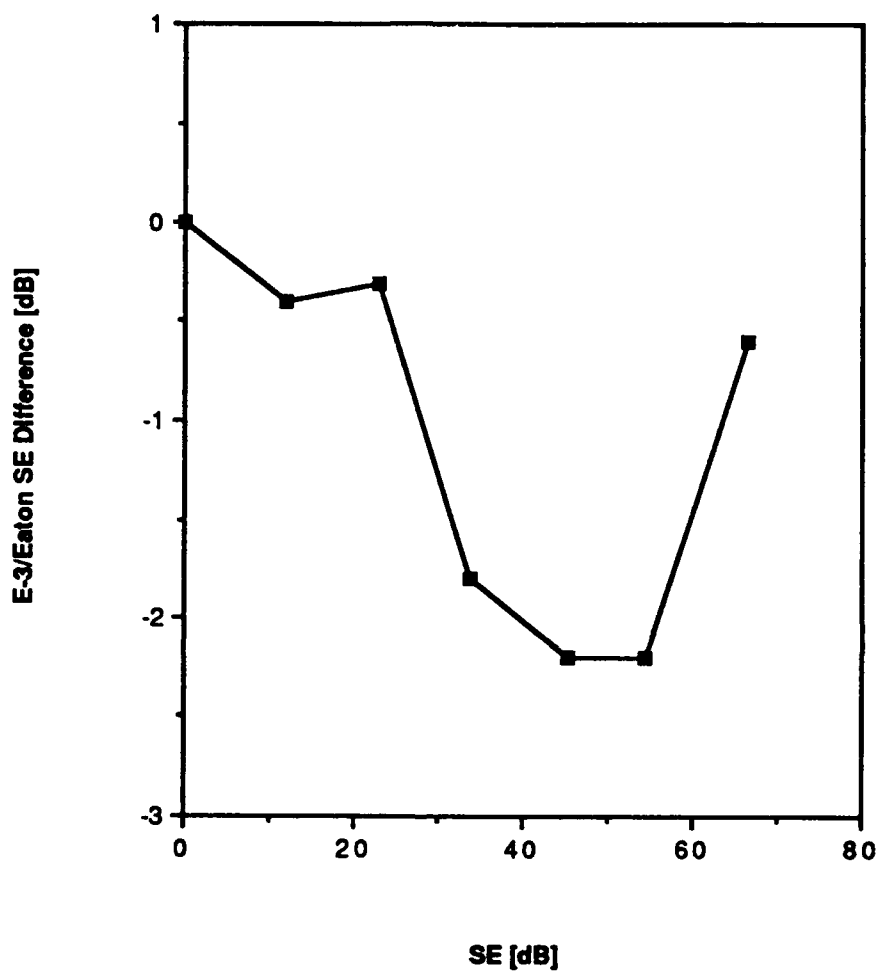


Figure 4.7 E-3/Eaton Linearity Comparison, 1.00 MHz

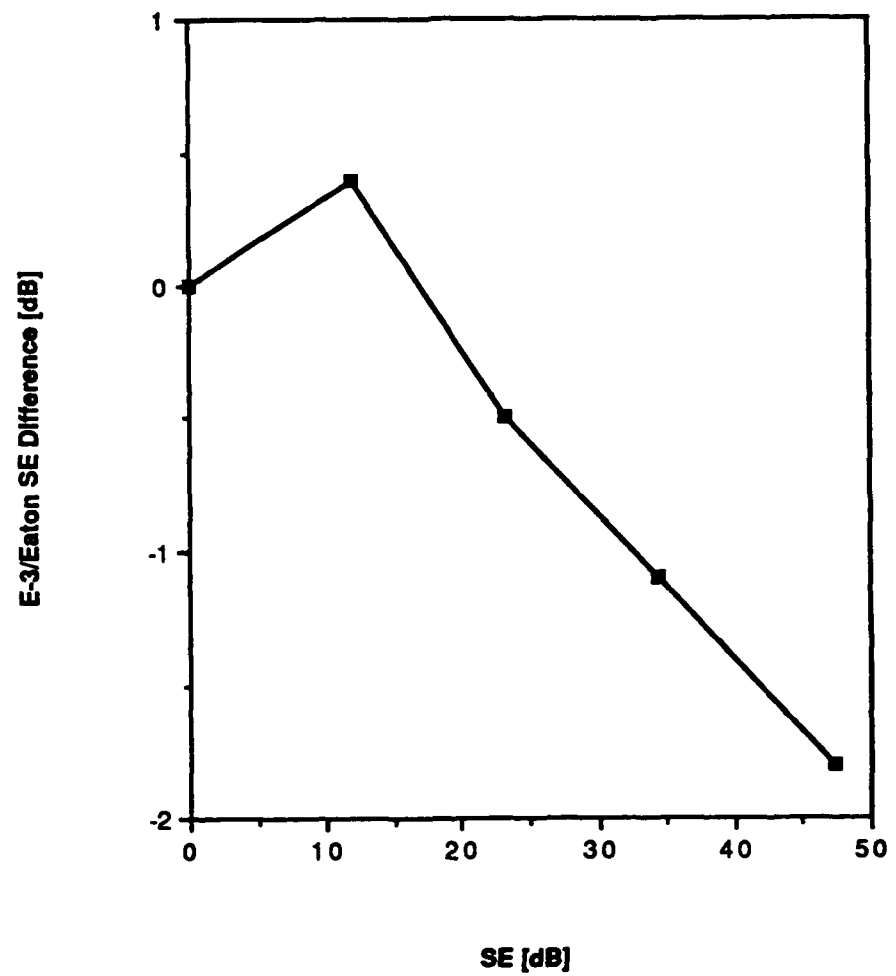


Figure 4.8 E-3/Eaton Linearity Comparison, 10.0 MHz

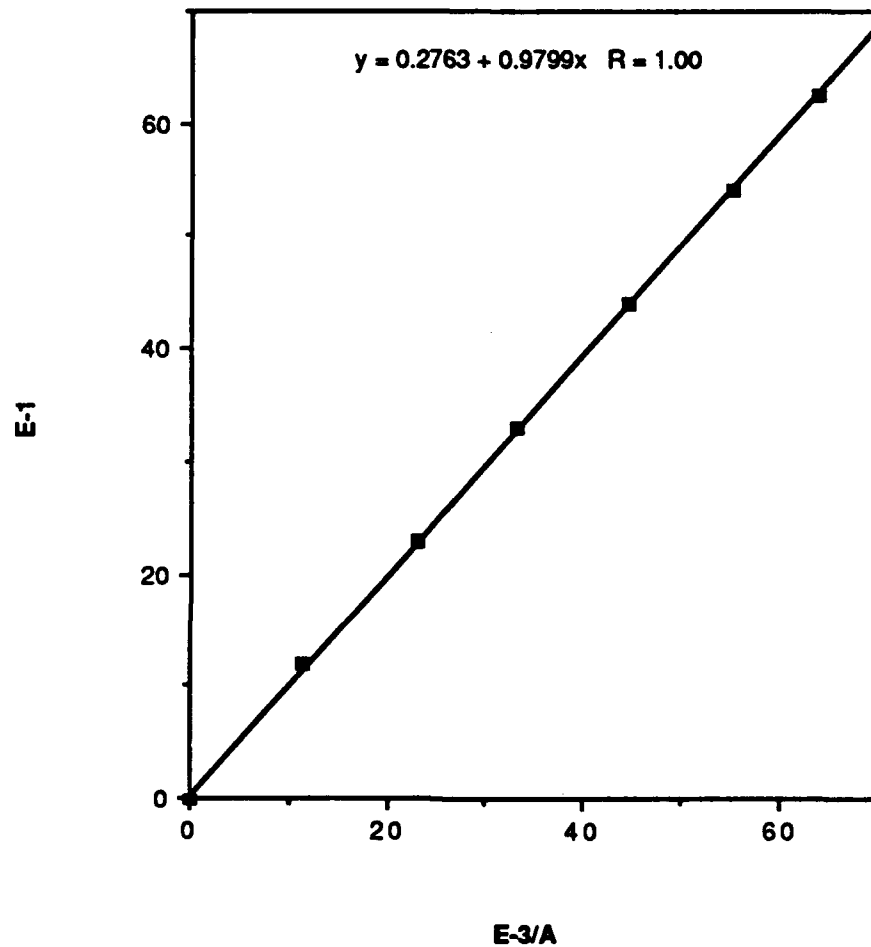


Figure 4.9 Comparison of E-1 to E-3

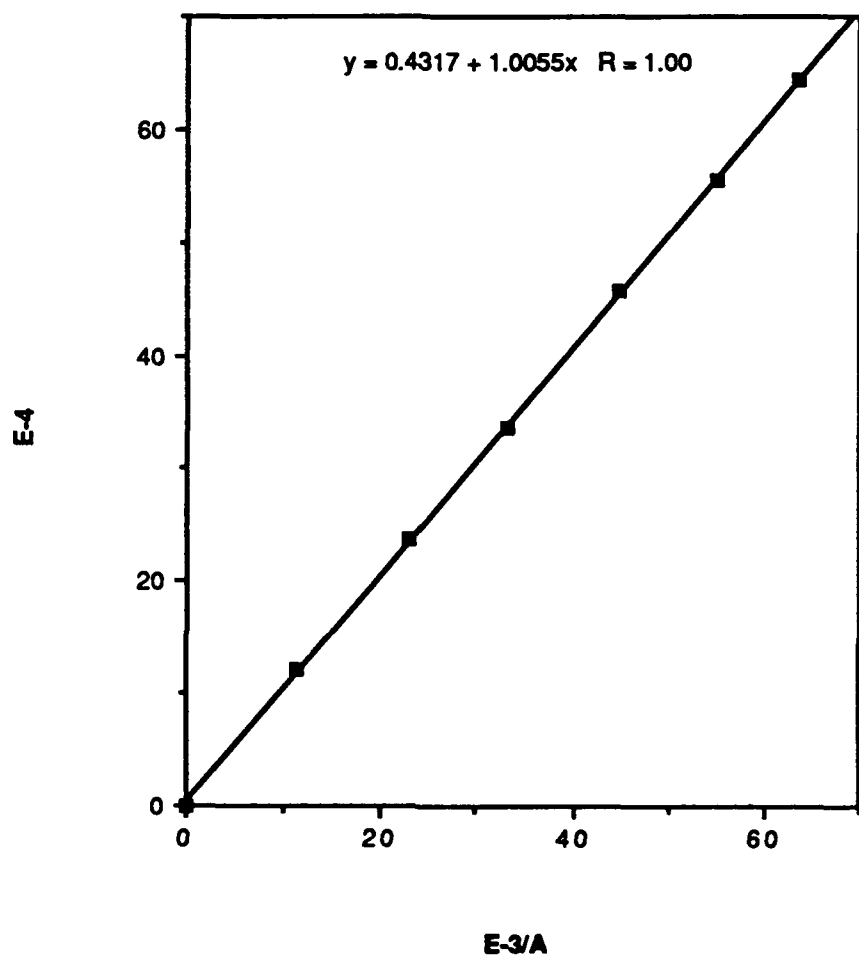


Figure 4.10 Comparison of E-4 to E-3

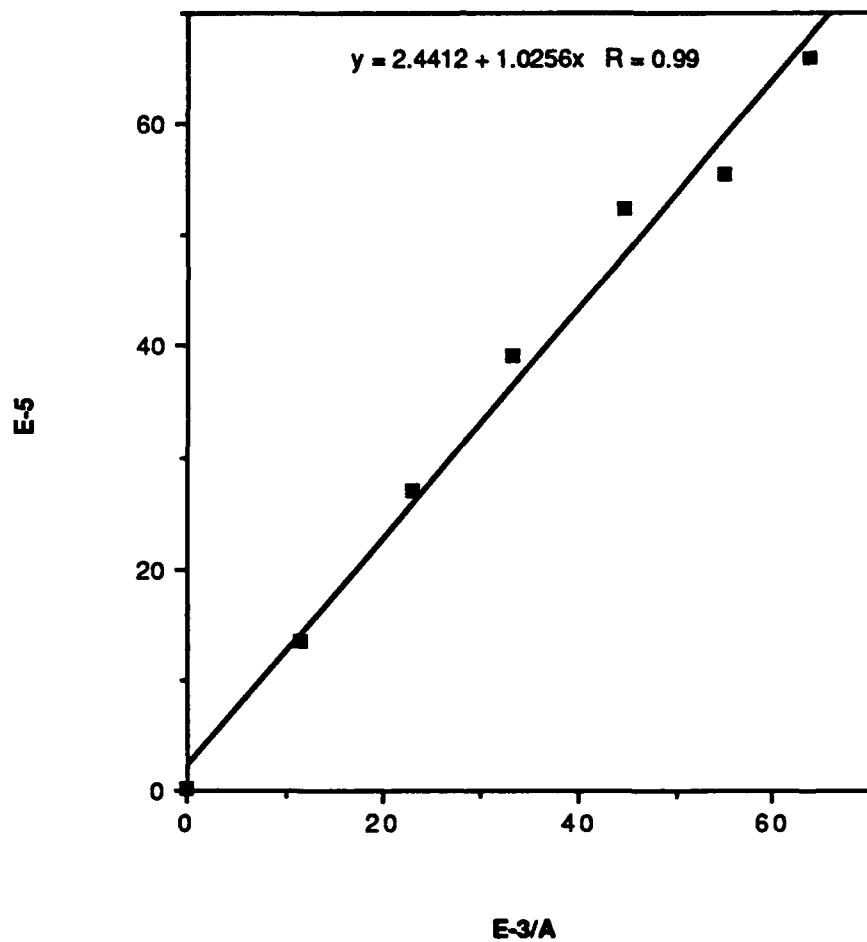


Figure 4.11 Comparison of E-5 to E-3

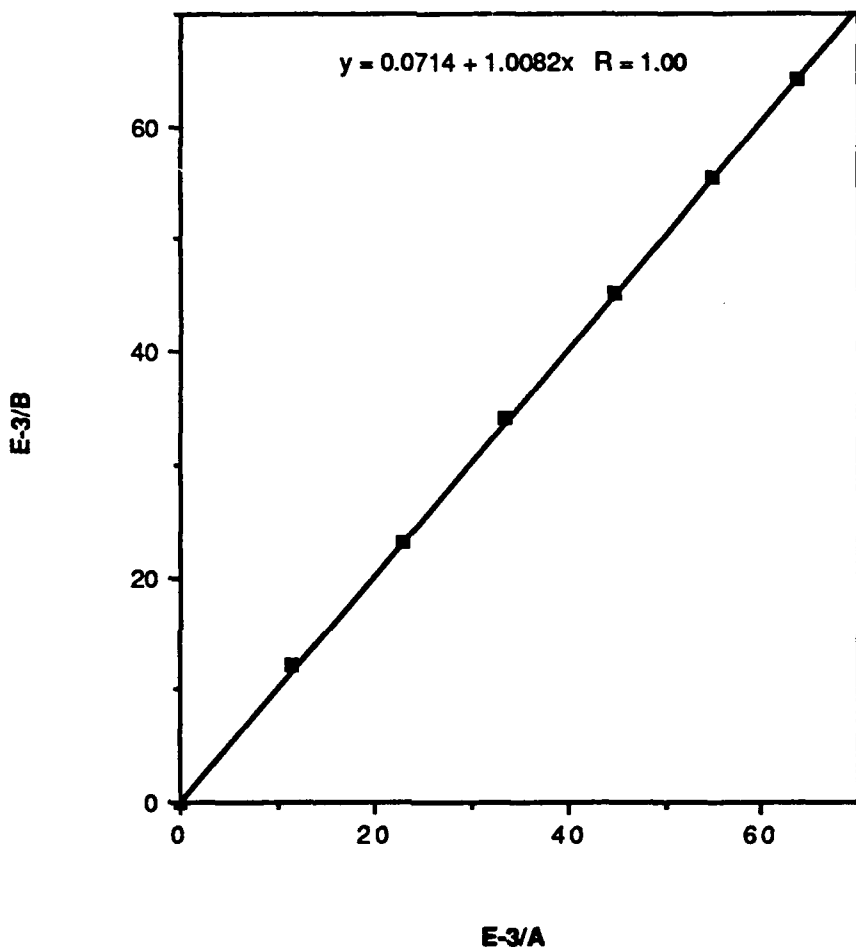


Figure 4.12 Comparison of E-3 to itself at Different Time

CHAPTER 5

MEASUREMENT REPEATABILITY

5.1 Repeatability of E-3 Measurements in a Precise Geometry

To determine the stability of the results from a given leak detector, a series of measurements were made using E-3. The test procedure described above, using different locations, was used. Six test locations were used at .156 MHz and 3 locations at the other frequencies. The measurements spanned several days, battery changes and temperature cycles. Figures 5.1-5.4 record the results. For the lower three frequencies over a SE range of 0 to 70 dB, the measurement spread is less than +/- 2 dB. At 10 MHz the spread is larger (+/- 4.5 dB at worst). 10 MHz is getting to be a rather high frequency for magnetic loop measurements because of wavelength and loop impedance effects. Furthermore, it must be admitted that the test procedure for this particular measurement was somewhat sensitive to operator position and other factors at 10 MHz. Therefore, it cannot strictly be concluded that the deviations are actually those of the Euroshield instruments.

5.2 Variations of Shelter SE Measurements

In addition to the previously described measurements in which the distance between transmitter and receiver was used to set the effective SE value, measurements were also made at six points on EMA's shielded enclosure. These points were chosen to give a range of SE values and measurement geometries. All of the four Euroshield leak detectors were used. The Eaton NM 17/27 receiver was used with an oscillator and two different power amplifiers (.010 - .250 MHz and .200 - 150 MHz). The operators of the transmitters and the receivers were also varied and measurements were taken over several days.

The results of this exercise are not nearly so tidy as those previously shown. Figures 5.5-5.8 demonstrate a considerable spread among the various SE's measured at each test point and frequency combination. In the best case the measurement variation is +/- 2 dB, but it becomes as large as +/- 7 dB. While the spread of these multiple measurements is, perhaps, disappointingly large, it is in the mainstream of MIL-STD-285 measurement variations.

Measurements with the Euroshield units in a well controlled configuration have been shown to be quite repeatable (Section 5.1) and the Euroshield units correlate well with each other and with other calibrated receivers (Sections 4.1-4.2). However in practical SE measurement on typical shelter test points with different operators, the variations can be as large as those obtained with other instrumentation.

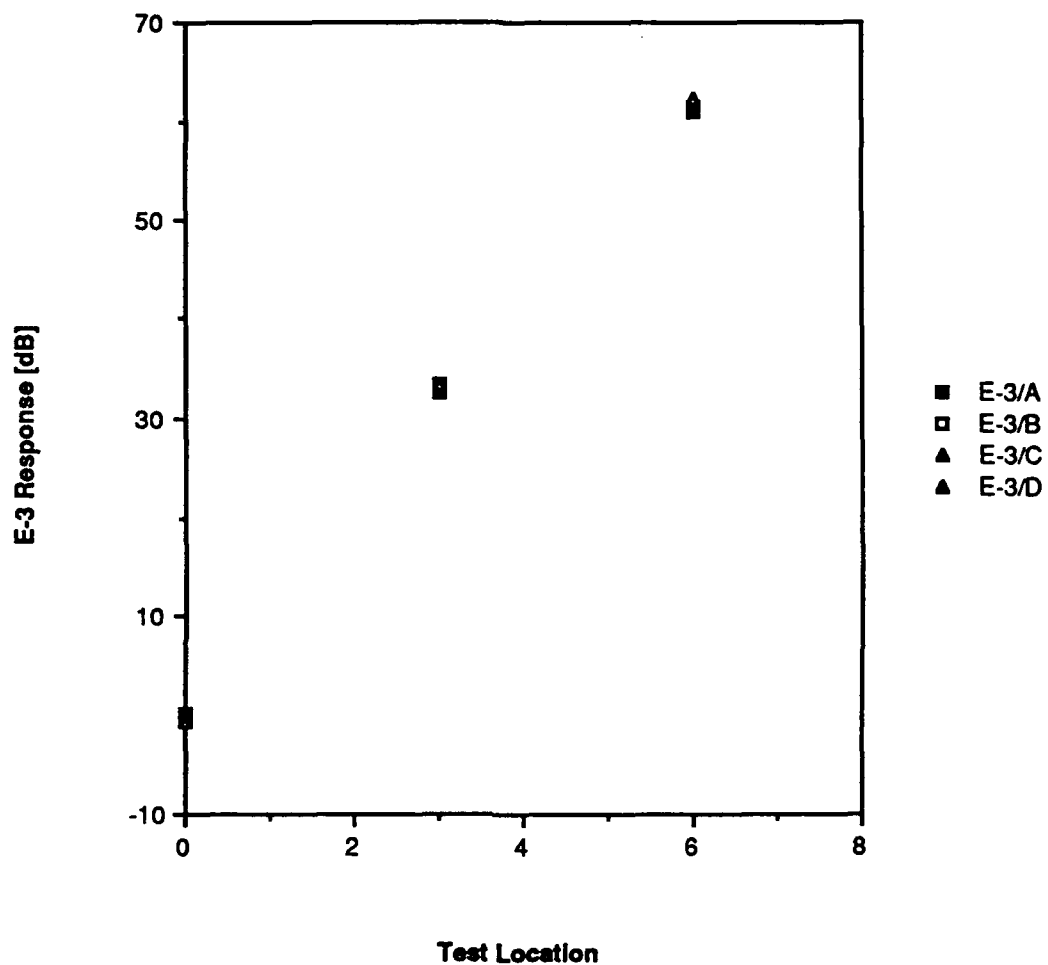


Figure 5.1 E-3 Repeatability Comparison, Separation at .010 MHz

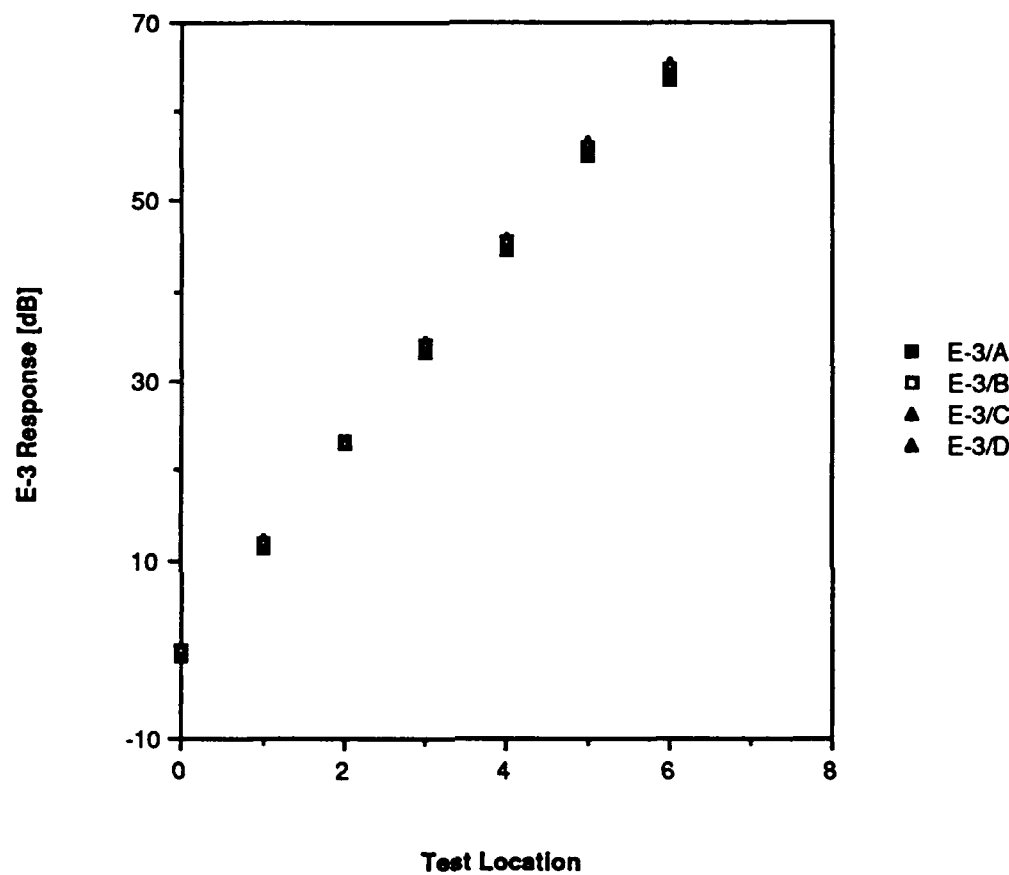


Figure 5.2 E-3 Repeatability Comparison, Separation at .156 MHz

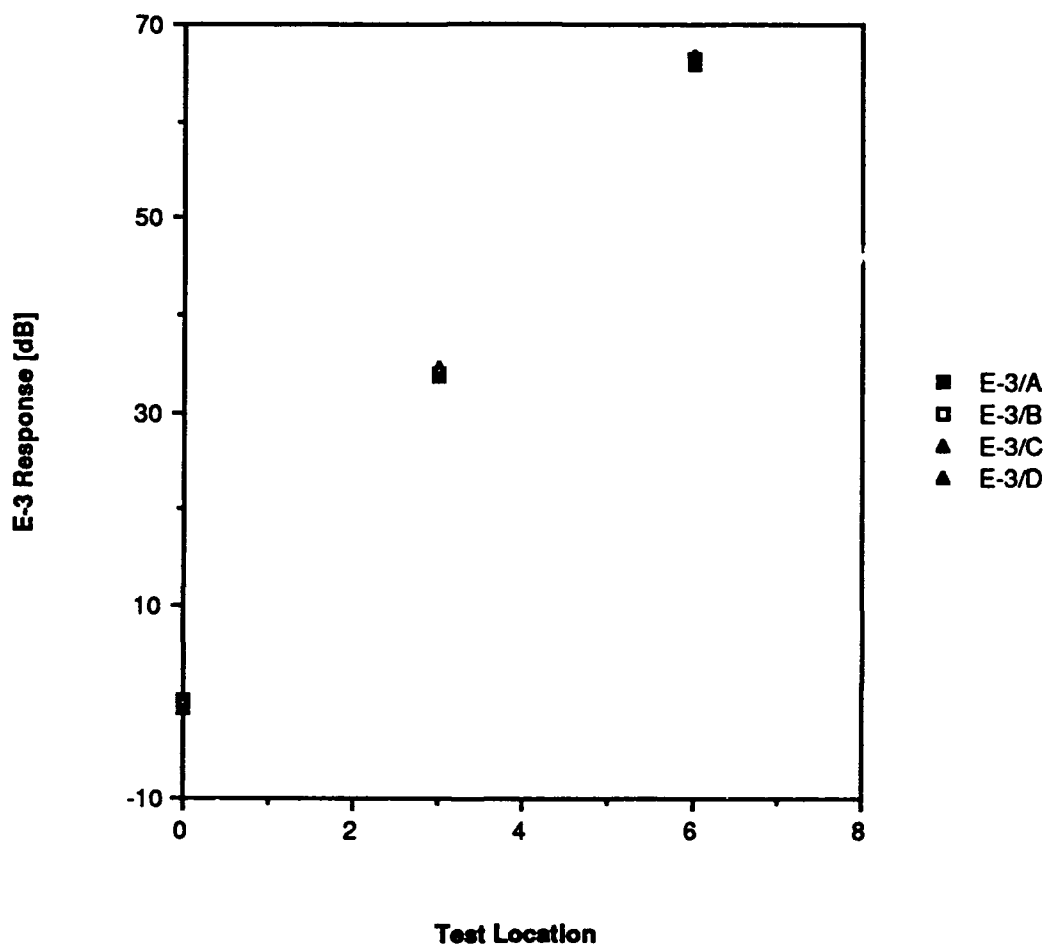


Figure 5.3 E-3 Repeatability Comparison, Separation at 1.00 MHz

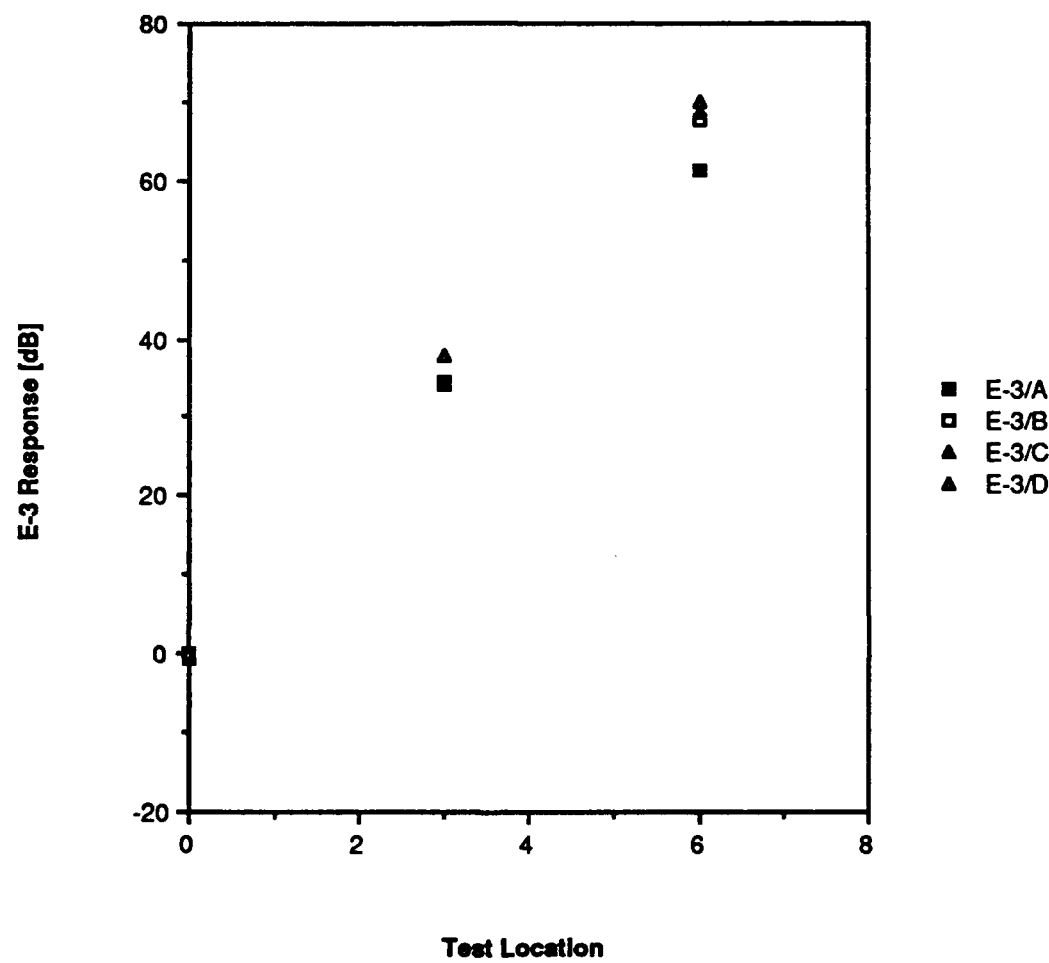


Figure 5.4 E-3 Repeatability Comparison, Separation at 10.0 MHz

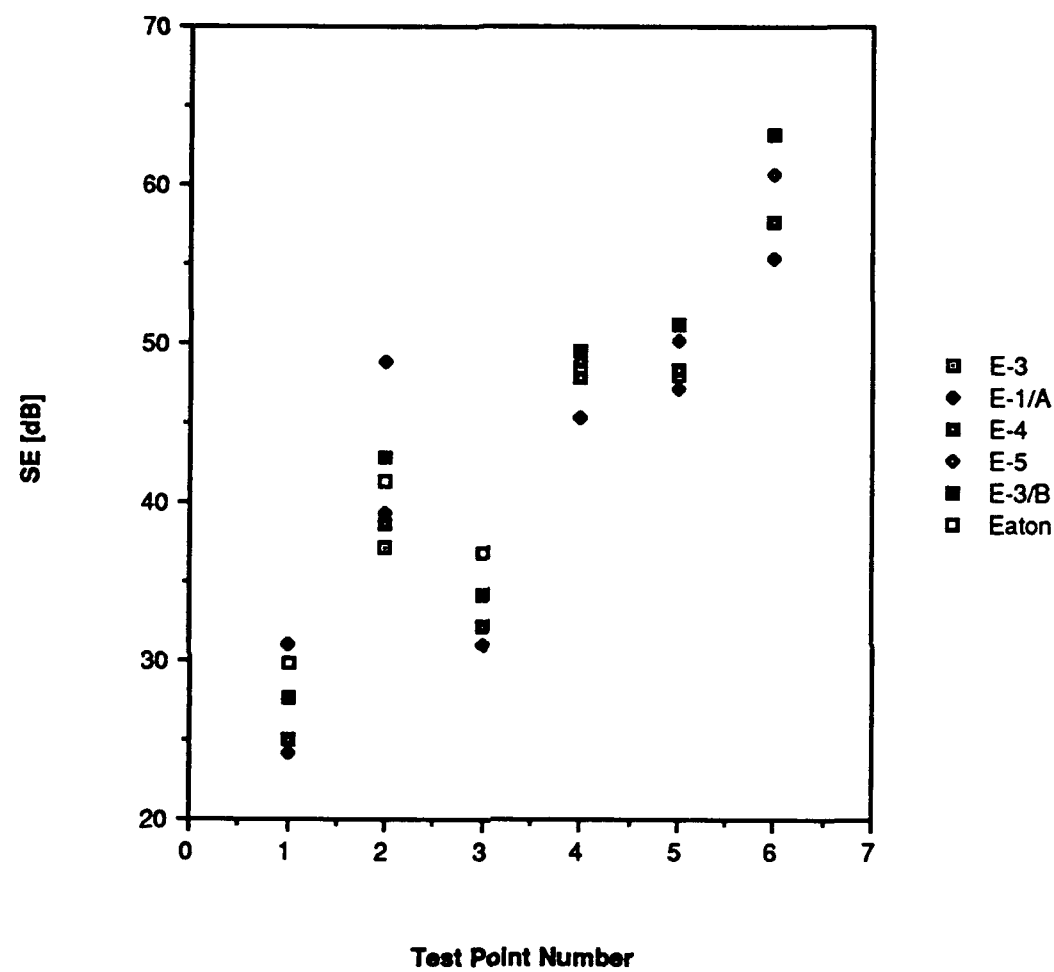


Figure 5.5 SE Comparison, .010 MHz

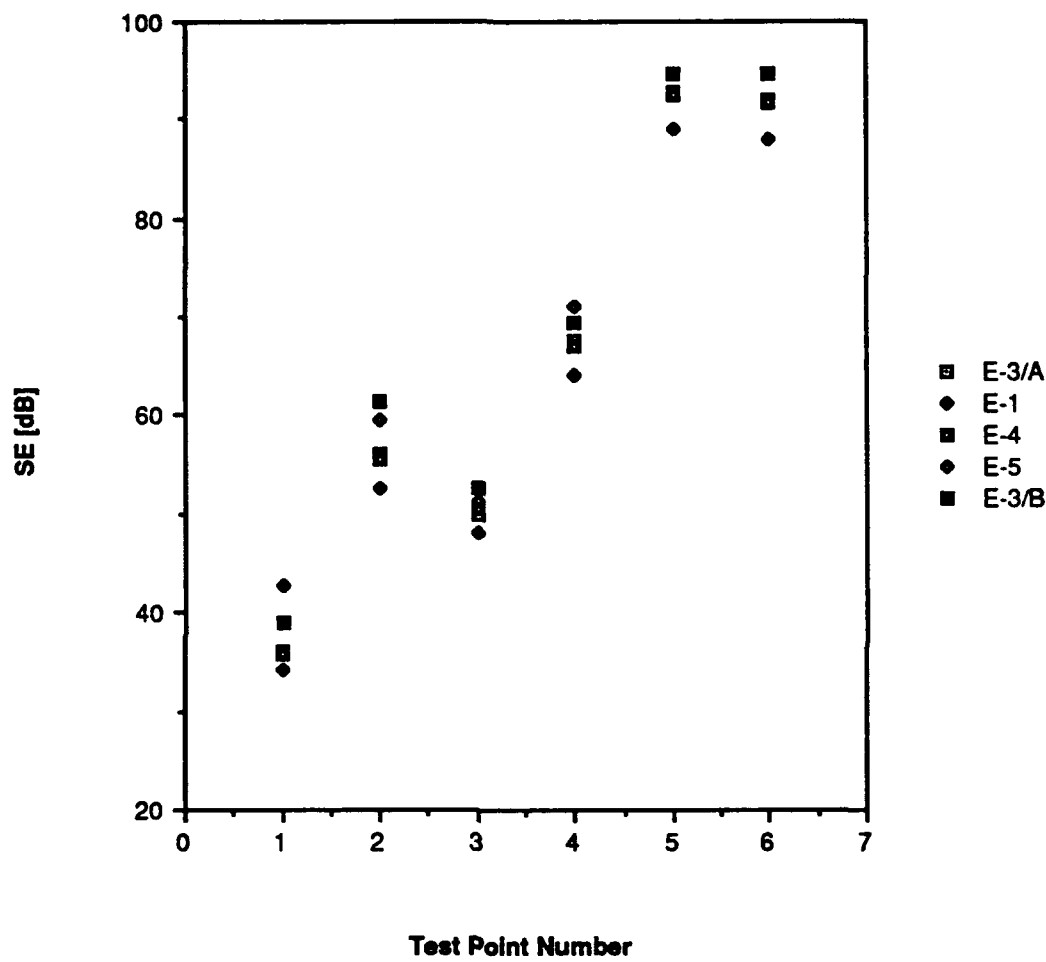


Figure 5.6 SE Comparison, .156 MHz

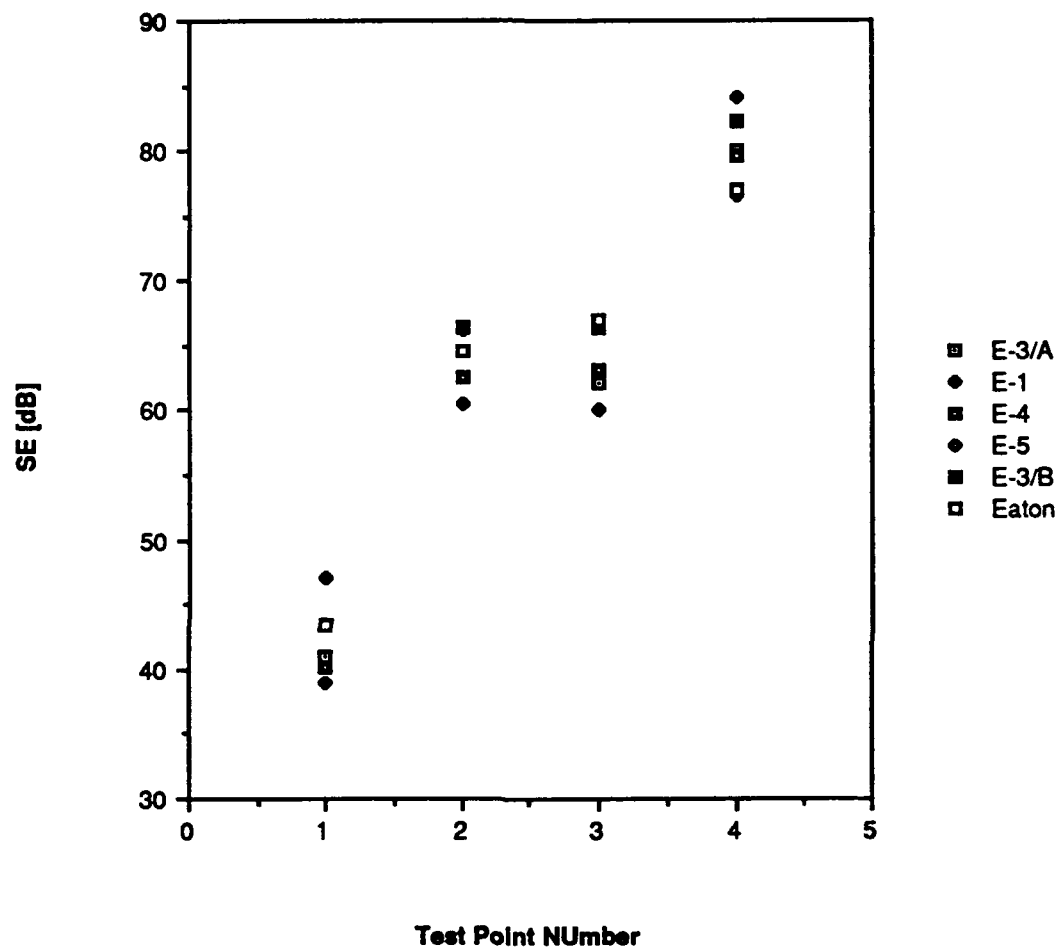


Figure 5.7 SE Comparison, 1.00 MHz

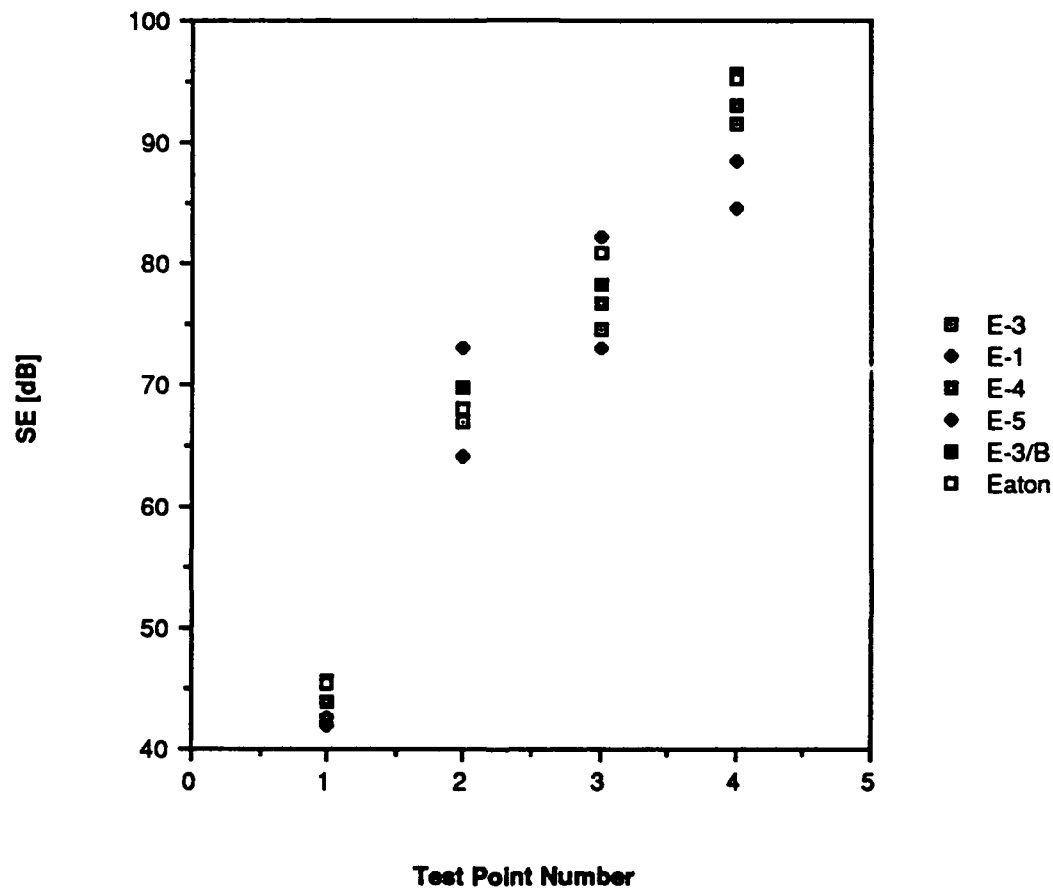


Figure 5.8 SE Comparison, 10.0 MHz

CHAPTER 6

IMPACT OF ENVIRONMENT UPON MEASUREMENTS

Nearly all of the measurements presented up to this point were made at room temperature and relative humidity, typically ~ 25 C and ~ 40% RH. The manufacturer's specifications are an operation range of 0 to +40 C and a storage range of -5 to +45 C. For our studies, extreme values outside the operating range were chosen, -12 and +45 C. These were deemed acceptable extensions which would probably not permanently damage the instruments.

To exercise the Euroshield leak detectors over a wider temperature/humidity range, an environmental chamber (Tenney) was used (the same one use to qualify the digital readout units). For this study, the E-3 transmitter and receiver were used. The units were opened up and the batteries removed. They were then placed inside the chamber and the temperature and humidity was selected. Time was allowed for equilibration of the leak detector to the specified temperature and humidity. This ranged from a few hours for the higher temperatures to >16 hours for the lower temperatures. The environment combinations are listed in Table 6.1

Table 6.1
Temperature - Humidity Combinations

Temperature degrees C	Relative Humidity %
-12	100
0	100
25	40
45	10
45	85

The measurement procedure after environmental stabilization called for:

- the removal of the units from the Tenney chamber
- the reinsertion of batteries and sealing of the units
- the turning on of the transmitter and receiver
- the elapse of ~2 minutes for circuit warm-up
- free field calibration
- measurement of SE at different transmitter/receiver separations
- measurement of SE at different test points on EMA's shielded enclosure

The first set of separation measurements could typically be completed within 10 minutes and all measurements could be completed in 15 minutes. The short time span from removal from the environmental chamber to completion of the measurements offers some hope that the instrument interiors were in the states defined in Table 6.1. Of course, this is less true for humidity, as condensation was observed to occur on the cold units and the high humidity at 45 C was probably rapidly lost to the relatively dry room temperature air.

The frequency focus of the temperature/humidity study was .156 MHz. All the shelter measurements were made at this frequency. For the separation SE measurements, two locations in addition to the calibration position were used. Figures 6.1-6.4 exhibit the SE evaluations made at common separations for all temperature and humidity combinations. The clustering of measurements is amazingly tight, especially considering that some of the low temperature measurements were made only three minutes after removal from the Tenney chamber. The shielding effective measurements made at the six test points on the shielded room agree nearly as well. This is true for SE values of nearly 100 dB.

Usually large dynamic range for fixed frequency SE measurements is achieved by employing a narrow bandwidth receiver and precisely tuned, stable oscillators for both transmitter and receiver. Such oscillators are vulnerable to drift under the influence of temperature change. Indeed the Euroshield leak detector User's Guide recommends a maximum temperature variation of 3° C. The leak detectors certainly function well over a wide temperature range. Recalibration might be necessary if the units undergo significant temperature change while in use.

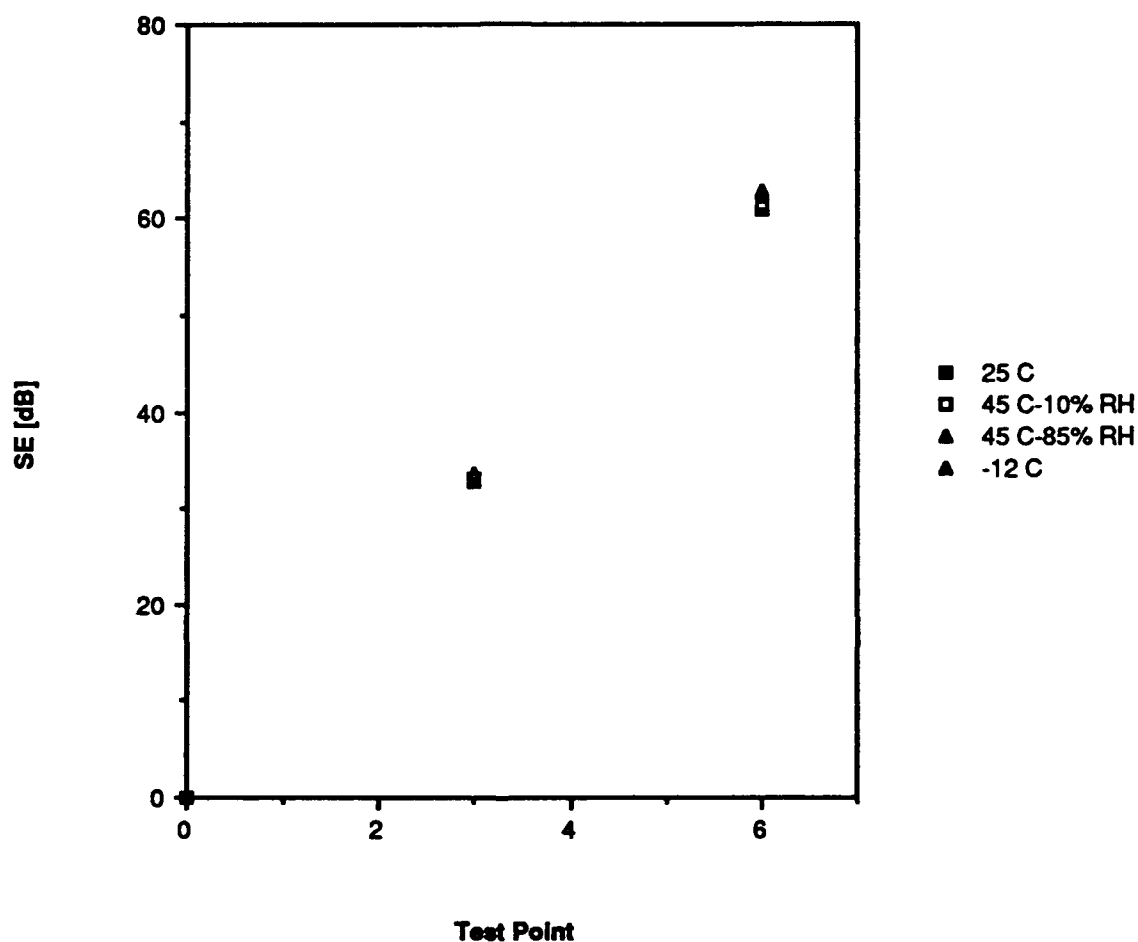


Figure 6.1 Temperature Dependence, .010 MHz

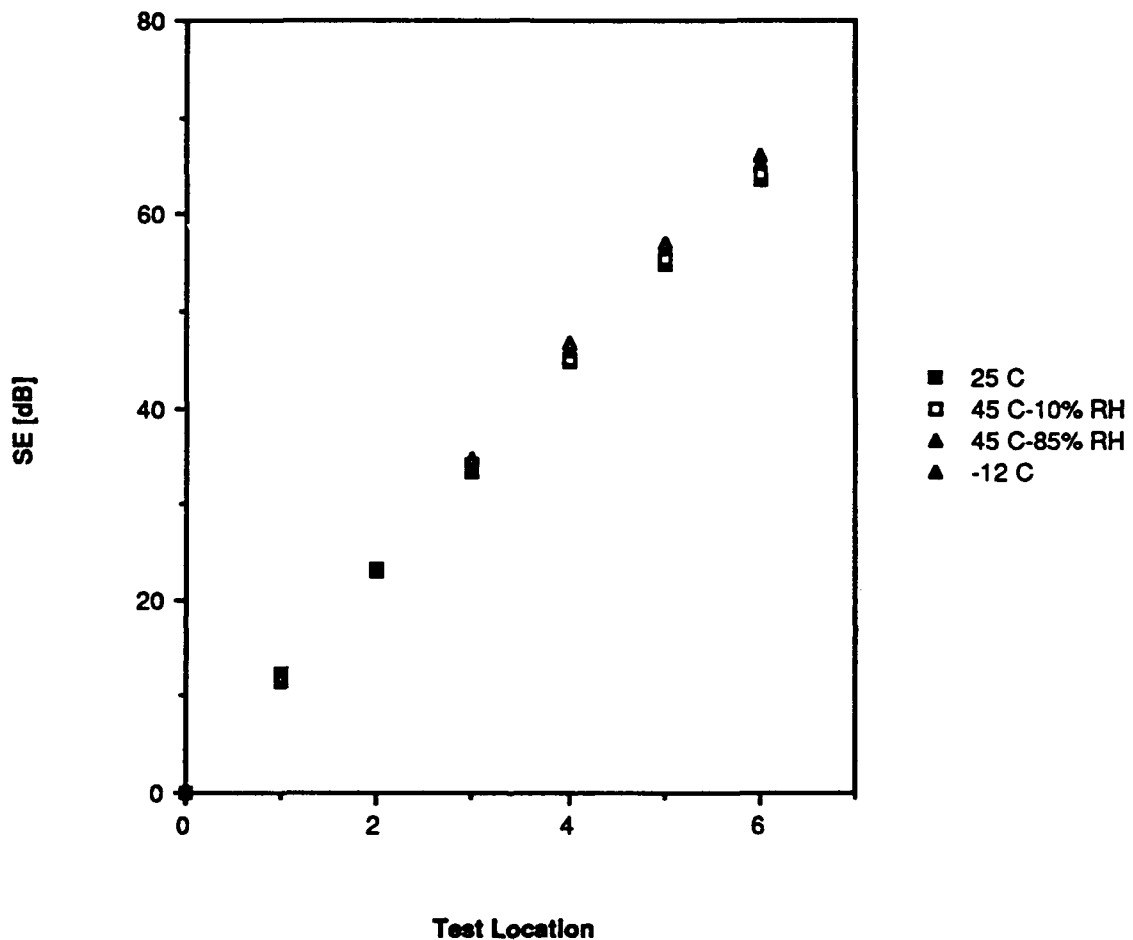


Figure 6.2 Temperature Dependence, .156 MHz

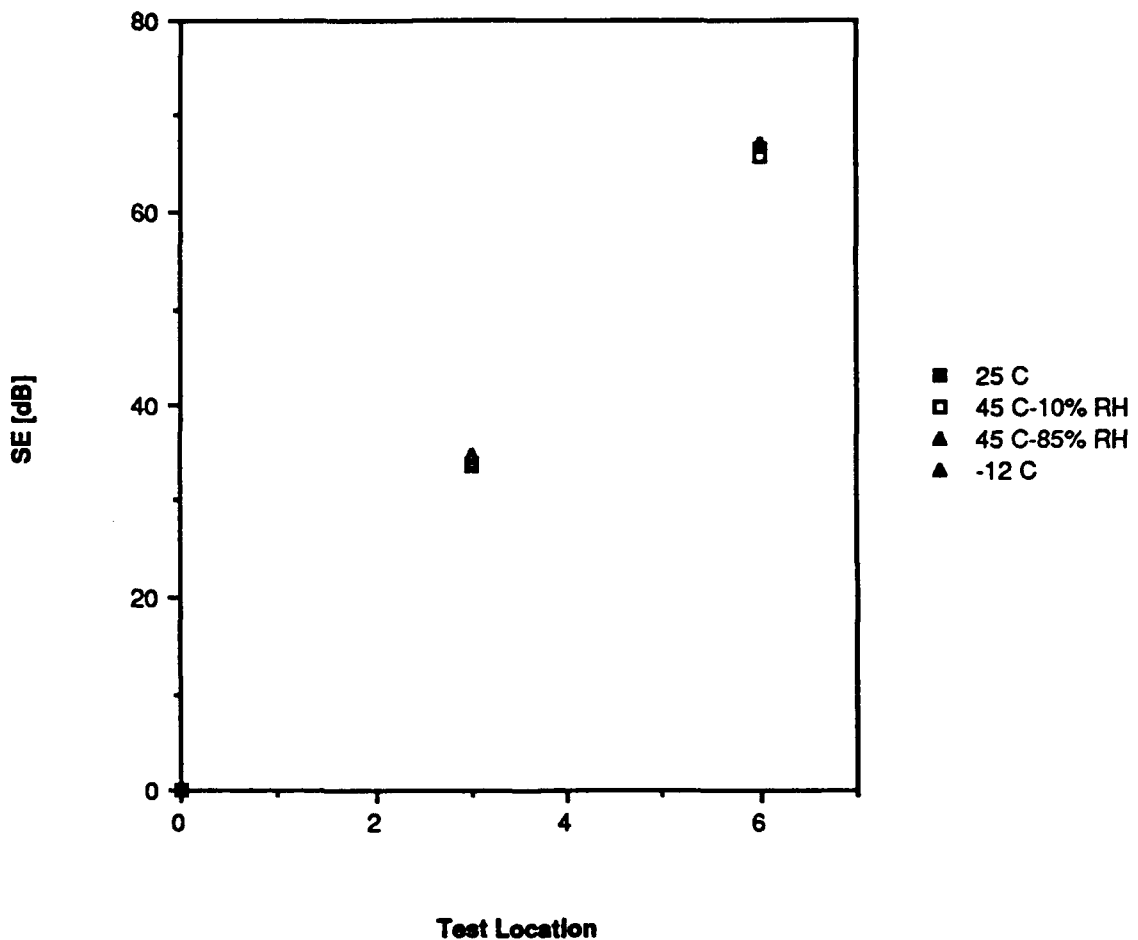


Figure 6.3 Temperature Dependence, 1.00 MHz

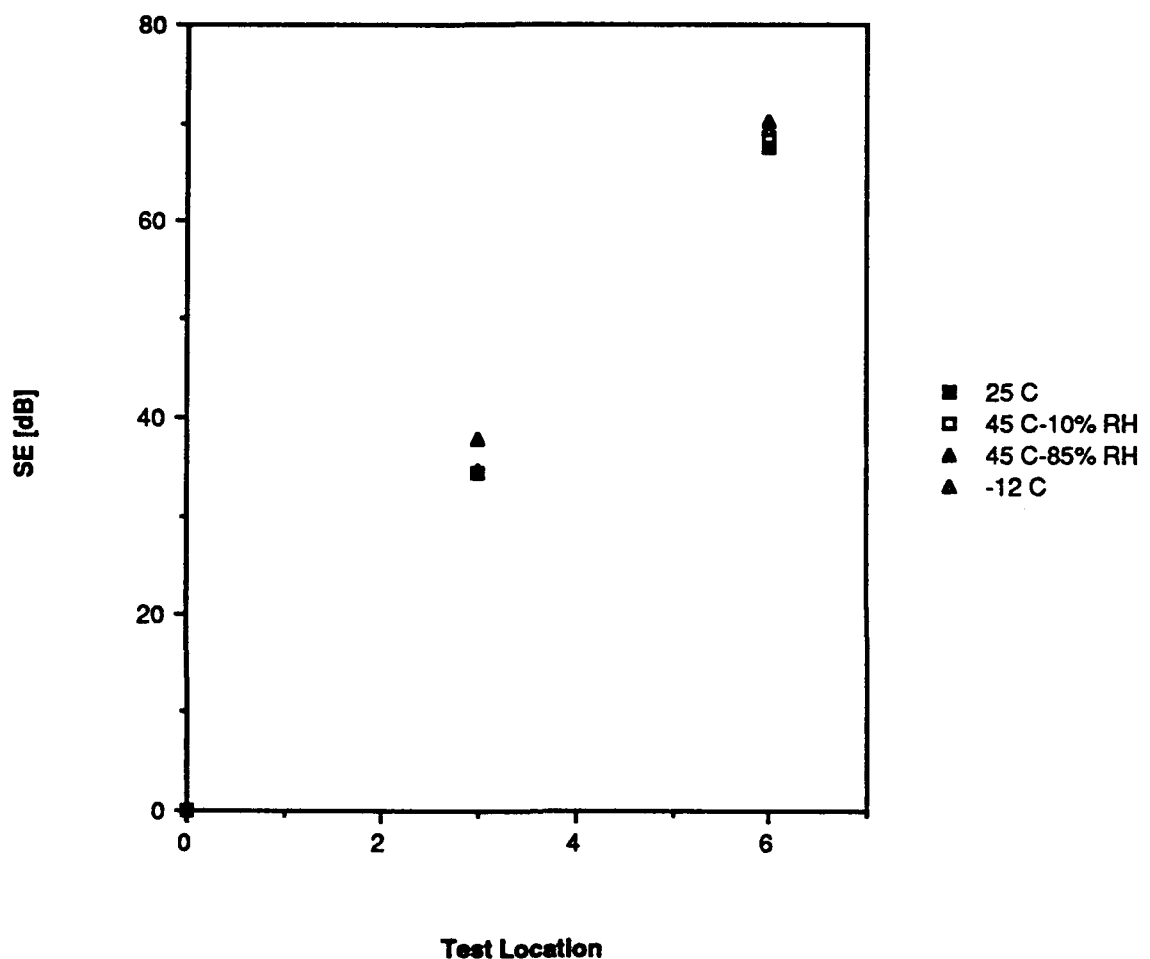


Figure 6.4 Temperature Dependence, 10. MHz

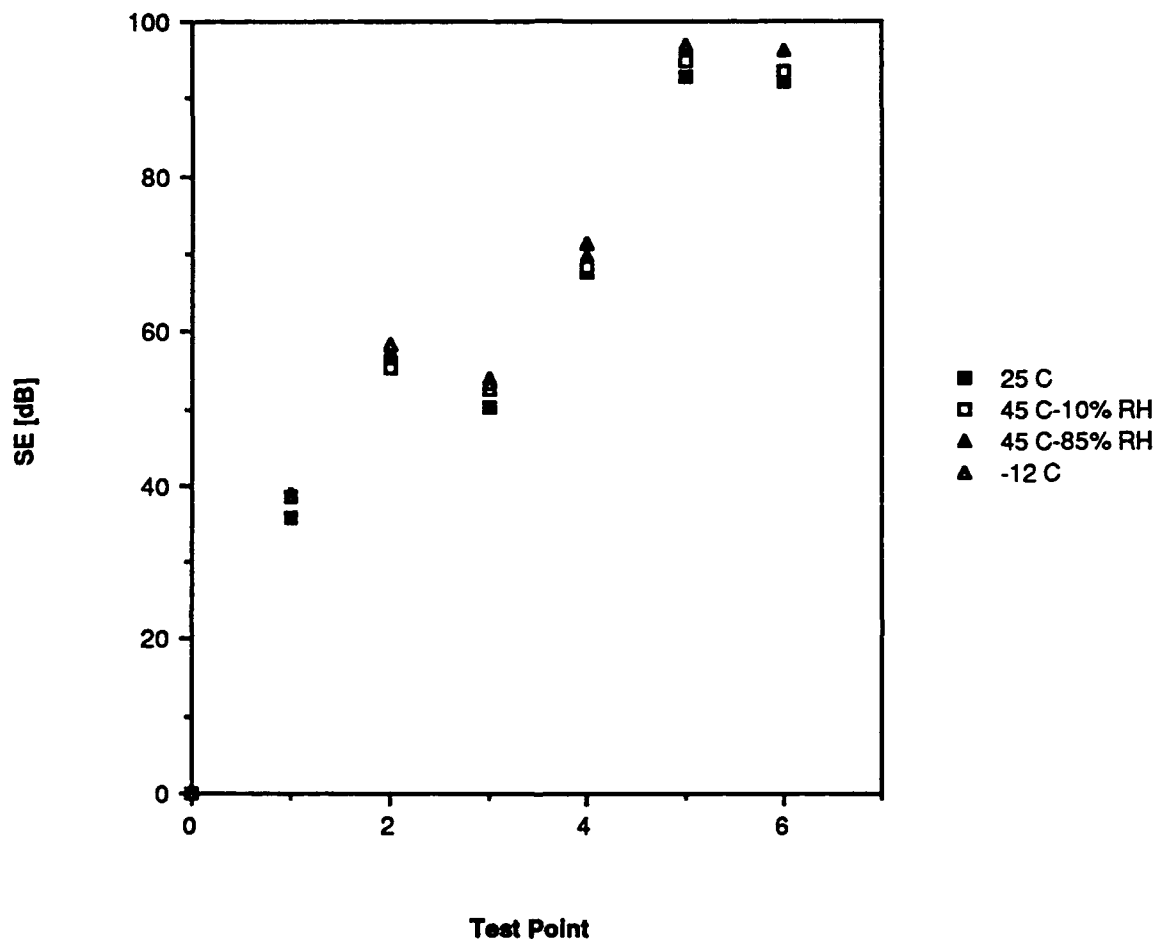


Figure 6.5 Temperature Dependence, Shelter at .156 MHz

CHAPTER 7

SUMMARY AND CONCLUSIONS

7.1 Summary

A study was made of various performance characteristics of the handheld Euroshield RF leak detector 4F-130. These instruments function at four frequencies from .010 MHz to 10.0 MHz and can measure SE's up to 82 - 120 dB, varying by unit and by frequency. For most of the studies the .156 MHz frequencies was examined in most detail. As a precursor activity, a sample and hold digital readout was installed in each of the four transmitter/receiver pairs used in the study.

In a well constrained geometry, repeatability of measured SE values from a single detector set was quite good as was the agreement between different leak detection sets. In traditional MIL-STD-285 applications, the measurement spread diverged considerably to as much as +/- 7 in the worse case shielding effectiveness obtained with many differences in instrument system, operator, time and temperature.

The units performed well under environmental stress ranging from -12 C to +45 C and form 10% RH to 100% RH. For measurements, with calibration, made over a short time, there was no significant degradation of performance. This is true, even though the temperature range covered in testing exceeded both the specified operating and storage temperatures.

7.2 Other Observations

Despite the overall good performance of the Euroshield RF leak detectors, a few items should also be noted for the record.

1. The batteries are somewhat loose within the instruments, supported by copper coated springs. If the batteries bounce and power is momentarily lost in the receiver, recalibration is necessary. This is very frustrating to an operator in the middle of a set of measurement inside of a shelter. It can be remedied by the insertion of small spacers in the battery compartment.
2. Occasionally, there is a temporary difficulty with calibration. This was observed several times for unit E-5 at 10.0 MHz. Sometimes the use of another transmitter would allow proper calibration; at other times it would not help.

3. The input to the display driving digital to analog converted is neither uniform between receivers nor constant in a single receiver. For some units the digital input after calibration was 7 and for other units it was 8. Moreover, it was common for this input to change (usually increase) by 1 or sometimes 2 or 3 units within several seconds of the calibration initiation. The display increment corresponding to the lowest order bit change is .5 dB. A three unit change of 1.5 dB can be disconcerting at calibration time. For the most part, allowing a little settling time took care of the problem. Certainly, there is no need for concern or adjustment because of a calibration reading only 1 least count from zero.

7.3 Conclusions

The Euroshield RF leak detector 4F-130 is useful and reliable instrument. Its SE results do not significantly differ from those obtained by use of more costly and bulky equipment and its measurement range is comparable. With the addition of a sample and hold digital readout, the instrument is quite convenient to use. This is especially noticeable to an operator making comparison measurements using traditional MIL-STD-285 instrumentation.

APPENDIX A

IMPACT OF OPERATOR AND TEST GEOMETRY UPON MEASUREMENT

A.1 Operator Influence

During measurements using the Euroshield RF leak detectors, note was made of any possible systematic influence of the operator upon the measured SE values. In particular, the effect of operator proximity and orientation with respect to either the transmitter or receiver were carefully observed. Measurements were made with the units held by both operators and by dielectric fixtures. No significant effects could be discerned.

Only at 10 MHz at large free space separation between the transmitter and receiver could the operator location influence the SE reading. At this frequency, the separation was large enough that the near field component from the magnetic loop was no longer dominant. It must be remembered that, for SE measurement, this is an anomalous configuration in which the leak detector is not designed nor intended to operate.

There are, of course, operator idiosyncrasies which can affect SE measurement results but these are as individual as the operators themselves and are difficult to characterize systematically. It is hoped that the sample and hold digital readout may remove at least one source of error and bias in the shielding effectiveness measurement.

A.2 Calibration Location and Test Point Geometry Influences on SE

For the purposes of this discussion, it should must be noted that shielding effectiveness is not a fundamental electromagnetic quantity. It is a derived quantity which is determined nearly as much by the test protocol as by the intrinsic properties of a shelter. The type of antennas used, the excitation frequency, the size and type of apertures/penetrations and the internal and external geometry of an enclosure all can play important roles. In the rest of this section, one aspect of these will be considered, the proximity of conducting planes to the transmitter or receiver antennas.

A.2.1 The Effects of Images

The MIL-STD-285 magnetic loop test is a relatively low frequency procedure which utilizes the near field ($\sim r^{-3}$) of a magnetic dipole. The loop size and separations are such that, as far as the receiving loop is concerned, the transmitting loop can approximately be treated as a point magnetic dipole source. With this in mind, in the presence of a conducting plane an image dipole is generated according to the usual rules of geometric displacement for images. From a consideration of the pseudovector nature of the magnetic field, or from a consideration of the boundary conditions for magnetic fields at the surface of a perfect conductor, two conclusions can be drawn:

1. Dipoles normal to the conducting plane have images of opposite polarity. By symmetry, the sum of the source and image fields exactly cancels at the surface of a perfectly conducting plane.

2. Dipoles parallel to the plane have images of the same polarity and the sum of the source and image fields at the interface is twice that of the source dipole.

Figure A.1 illustrates the effect of statement 1. in the context of a MIL-STD-285 transmitter loop and a receiver loop. The distance is the height of the plane of the two loops above the perfectly conducting ground plane. The response is expressed in dB relative to the response in the absence of a conducting plane. It rises from a large negative dB value near 0 height to almost 0 dB effect at 1 meter.

Figure A.2 show the consequences of statement 2. For loops with axes parallel to the ground plane the receiver response is double (6 dB) at 0 distance from the ground plane. At 1 meter the response is less than .5 dB different from the result in the absence of a conducting plane.

Figures A.3 and A.4 records measurements made in the same geometries described for the previous two figures. In this case the conducting plane was a copper sheet approximately 3 meters on a side. The absolute magnitudes are unimportant in these figures. All that matters is the variation with distance from plane. When the loop axes are perpendicular to the conducting plane, a typical variation of 25 dB is observed. In the parallel orientation, a typical response enhancement of 4 dB is noted. These measurements are in reasonable agreement with the calculated values shown in Figures A.1-A.2.

The same measurements were repeated using a concrete ground plane. Concrete usually equilibrates to the moisture content of the soil base and its conductivity reflects this moisture level. In Colorado the soil is relatively dry and hence the concrete conductivity may be assumed to be low. Figures A.5-A.6 plot the source plus image responses over the concrete surface. For the parallel axes configuration, the results are not much different from the copper sheet. The perpendicular axes results, however are much moderated and show only a 3 dB effect.

A.2.2 Calibration and Measurement

The lessons learned above have obvious implications for the free field calibration in MIL-STD-285. The loops should be at least a meter distant from conducting surfaces. Otherwise, depending upon the orientation of the axes, the free field response will be either enhanced or diminished with respect to its true value. This will adversely affect all SE values computed using the erroneous free field value.

Similar effects are observed when making SE measurements inside of an enclosure. In this case the seams and apertures excited by the external transmitter loop become the sources for the receiving loop. Naturally, they will have images since the very premise of a EM shelter includes good conducting surfaces. Since the image is displaced

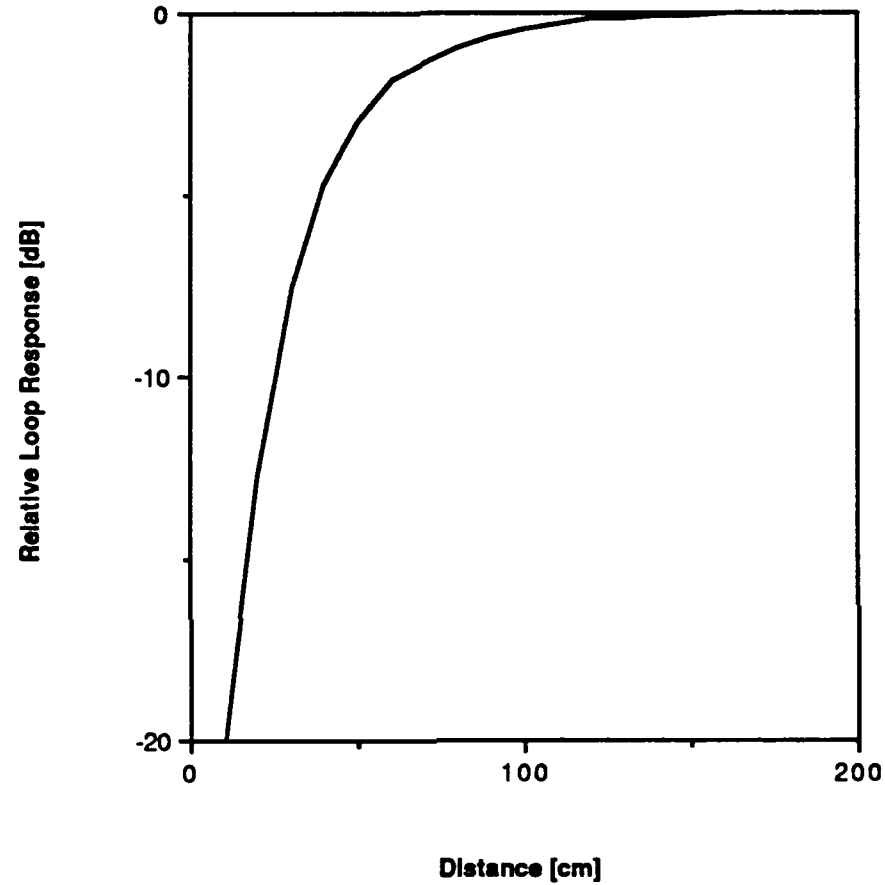


Figure A.1 Loop Perpendicular to Ground Plane, Theory

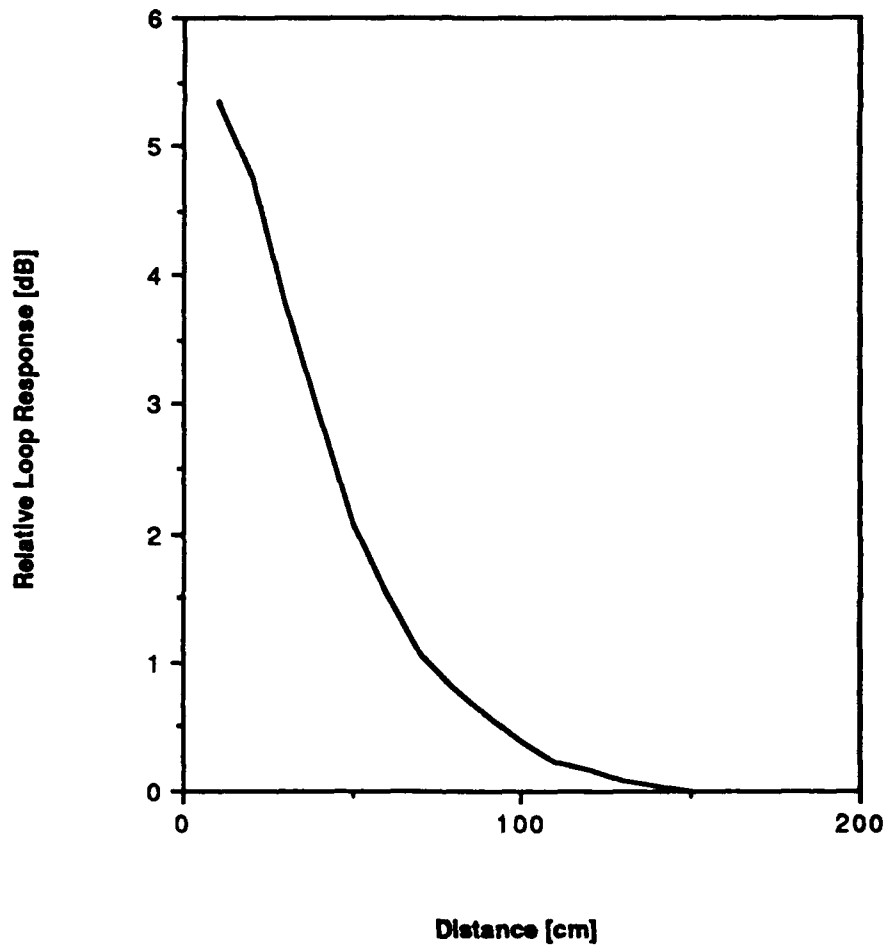


Figure A.2 Loop Parallel to Ground Plane, Theory

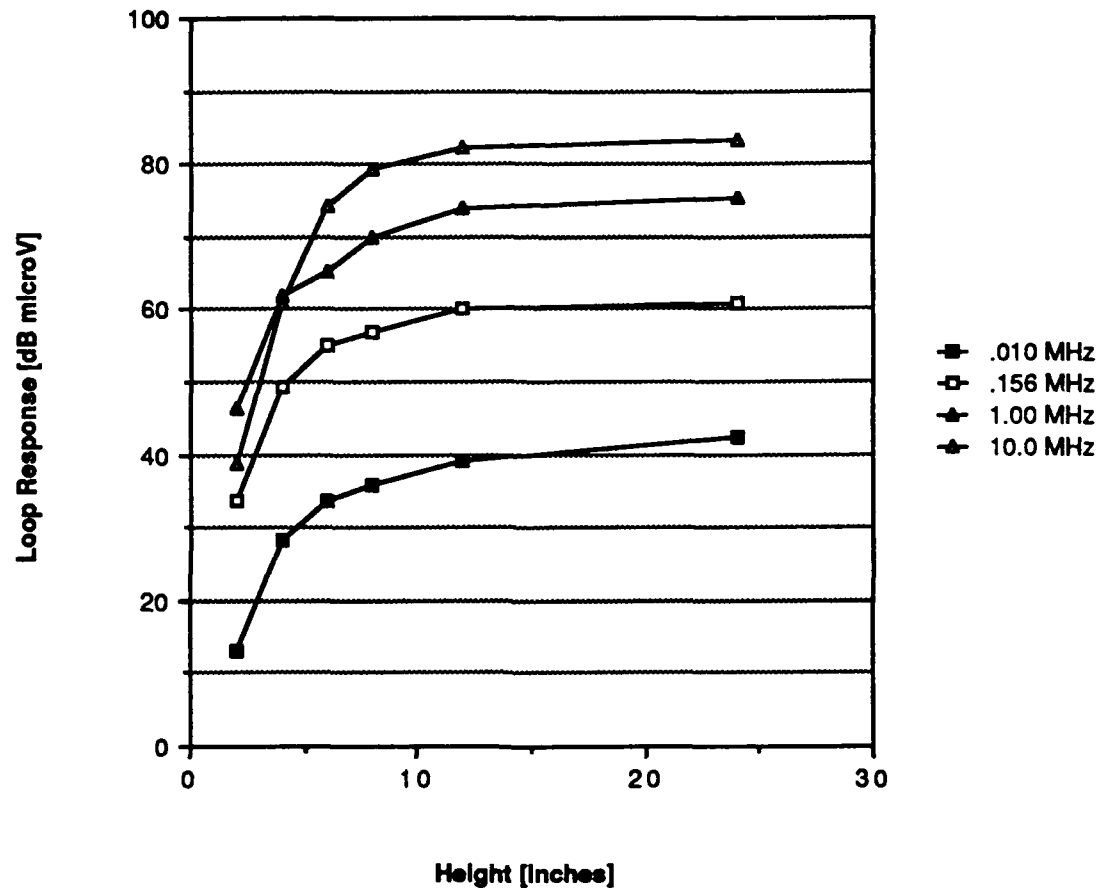


Figure A.3 Ground Plane Effects, Axes Perpendicular to Ground

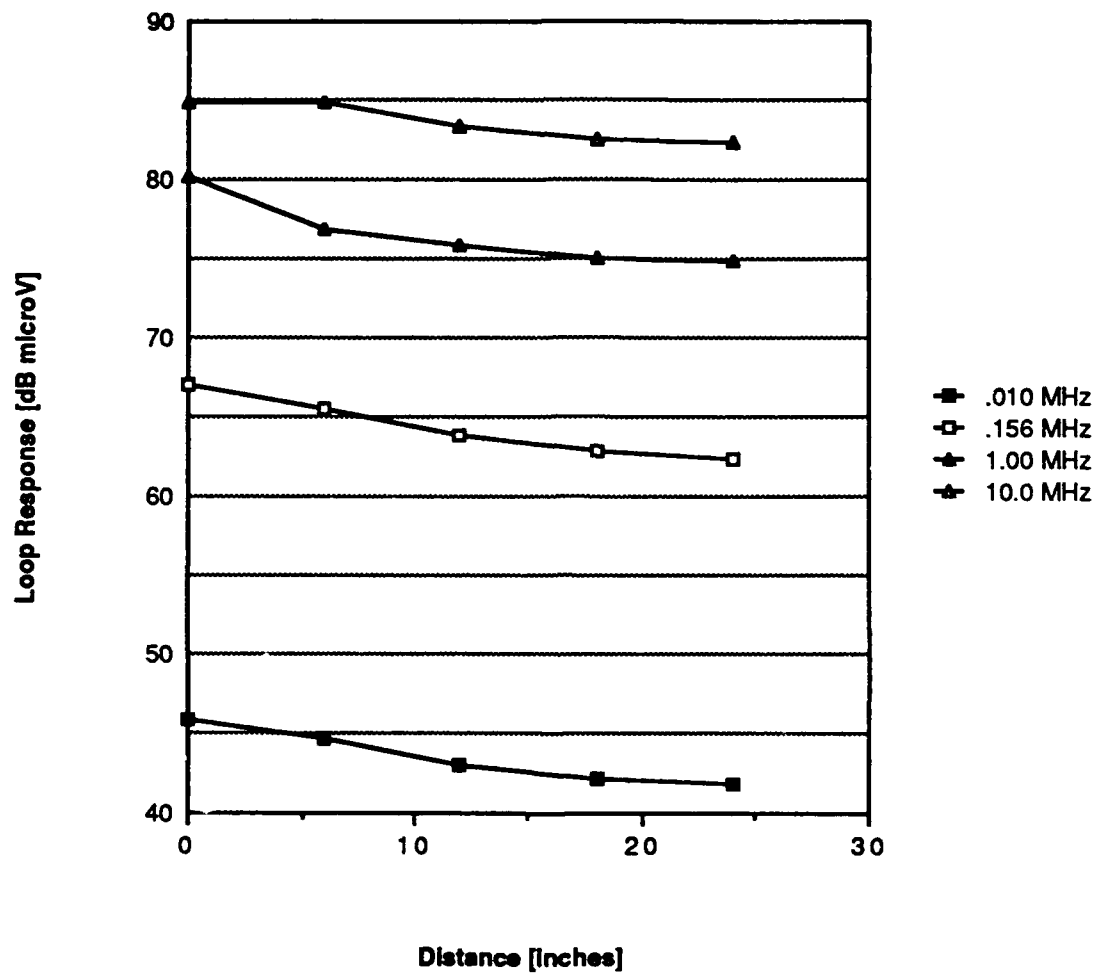


Figure A.4 Ground Plane Effects, Axes Parallel to Ground

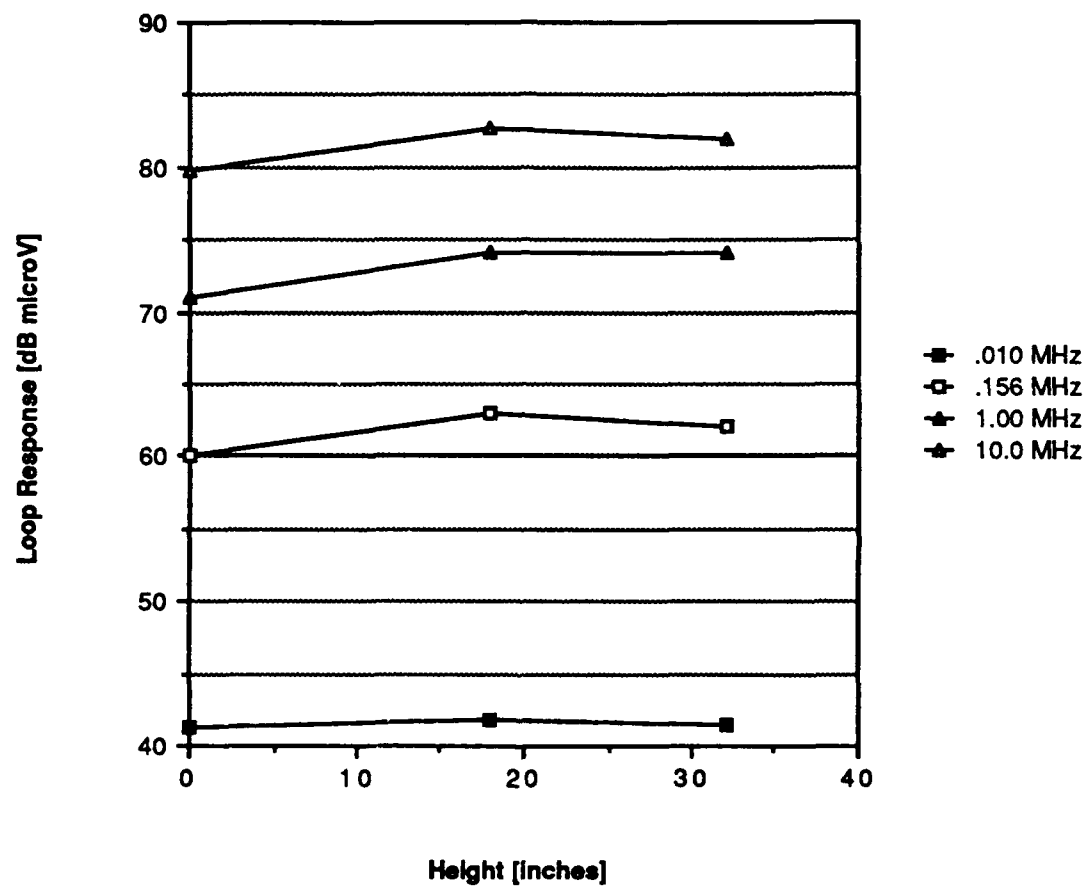


Figure A.5 Concrete Ground, Axes Perpendicular

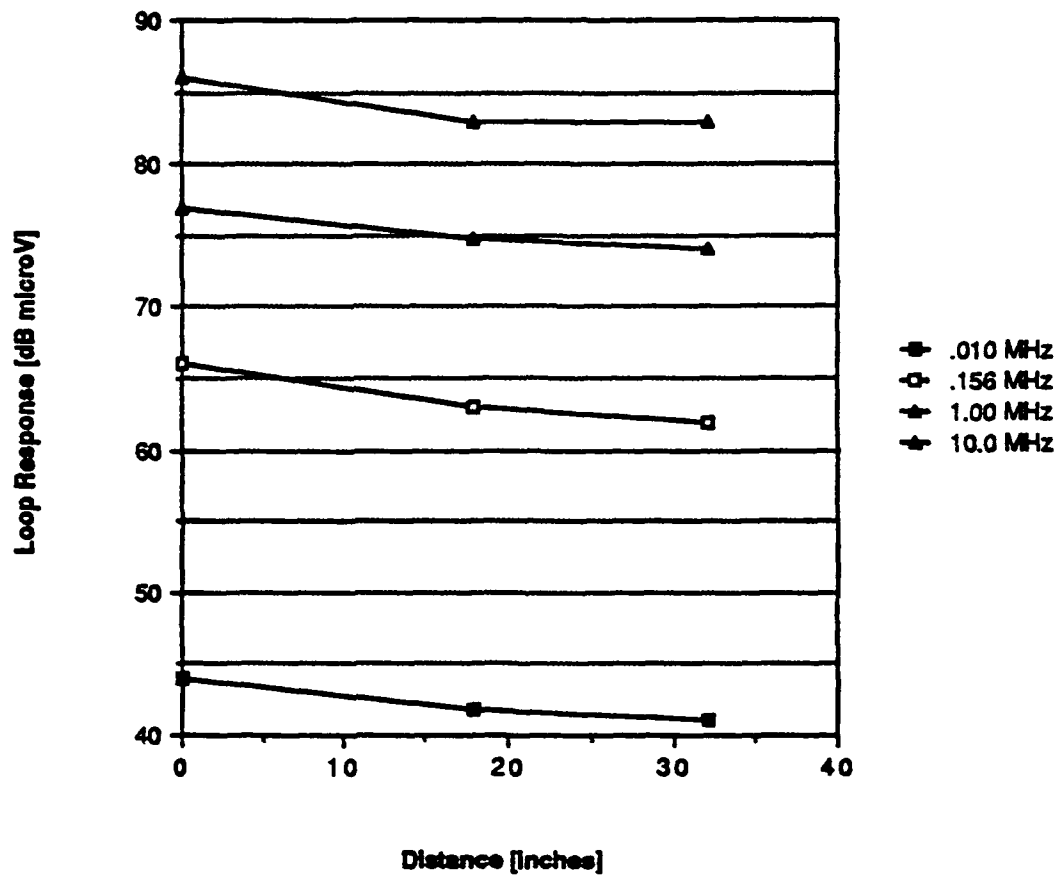


Figure A.6 Concrete Ground, Axes Parallel

an equal distance behind the conducting plane as the source is in front of it, only nearby surfaces are important (as seen in Figures A.1-A.4).

To test this model a set of measurements were taken along the two vertical door seams of EMA's shielded enclosure. A local source was generated by placing a six inch wide sheet of insulating polycarbonate in the door so as to prevent the finger stock from making electrical contact. This six inch sheet was moved, starting at floor level, upwards six inches at a time. For each position, an SE measurement was made at the center height of the polycarbonate sheet. This procedure was carried out on both the door latch side seam and the door hinge side seam. The former seam was at least 3 feet from another vertical plane whereas the door hinge side seam was only 3 inches from a vertical side wall. In Figure A.7 are the SE values so measured. Both of the previously discussed effects can be seen. For each side of the door, the receiver response was diminished (and the SE enhanced) when the measuring loop was near and with its axis perpendicular to the conducting floor plane. As the distance from the floor increased to near mid-shelter height, an asymptotic value was approached, just as in Figure A.1 (after flipping sign to go from SE to response). The hinge side response is also seen to be larger (SE smaller) just as in Figure A.2 but the quantitative agreement is mediocre after the first two points.

These measurements (Figure A.7) illustrate the complicated character of shielding effectiveness. At all points the same size gap was established by the polycarbonate sheet and the initial source for the interior excitation was the same at each point. Only the variations of the source with the internal and external geometry caused the difference in the measured SE's. Qualitatively, image theory can be used to explain some of the results.

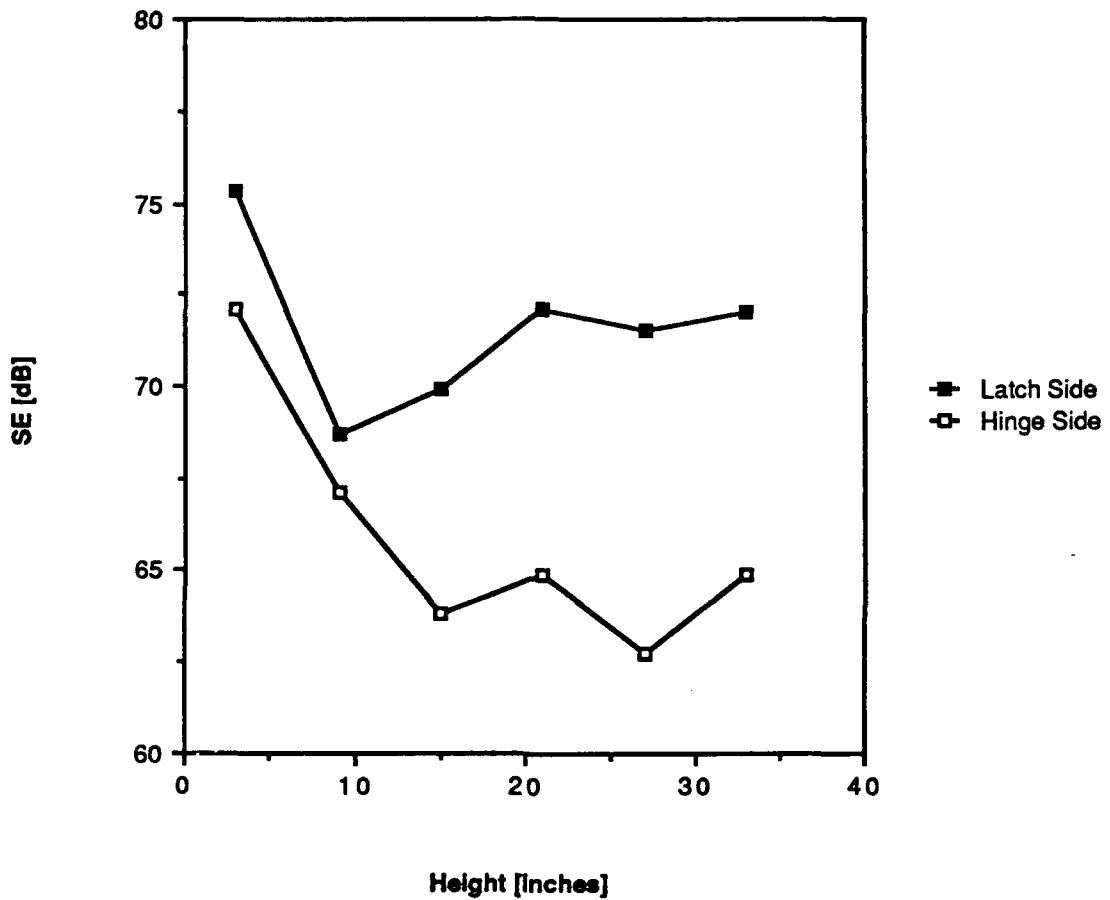


Figure A.7 Shelter Geometry SE Effect, .156 MHz